

Fidelity of alkenone paleotemperatures in southern Cape Basin sediment drifts

Julian P. Sachs

Department of Earth, Atmospheric and Planetary Sciences, Massachusetts Institute of Technology, Cambridge, Massachusetts, USA

Robert F. Anderson

Lamont-Doherty Earth Observatory, Columbia University, Palisades, New York, USA

Received 5 November 2002; revised 31 March 2003; accepted 16 May 2003; published 15 October 2003.

[1] Multiple geochemical analyses were performed in order to test the fidelity of alkenone paleotemperature reconstructions in southern Cape Basin sediment drifts. Sea surface temperatures (SSTs) derived from the alkenone unsaturation ratio, $U_{37}^{k'}$, in two drift cores (TN057-21 and Ocean Drilling Program Site 1089) are nearly identical during the interval of overlapping analyses, MIS 4-5c. SSTs in a nearby nondrift core (TN057-6) covary with those in core TN057-21 throughout MIS 1-5c. While climatological SSTs overlying TN057-21 and TN057-6 are similar and consistent with reconstructed Holocene SSTs in the nondrift core, surface waters overlying TN057-21 are $\sim 6^\circ\text{C}$ colder than Holocene alkenone SSTs in the drift core. Temperatures remain $\sim 6^\circ\text{C}$ warmer in TN057-21 relative to TN057-6 during the ~ 100 kyr duration of the records. We hypothesize that alkenone-derived SSTs in TN057-21 are higher than climatological SSTs in the overlying surface water and those in TN057-6 as a result of the winnowing and focusing of sedimentary alkenones produced in warmer waters to the north. Climatological SSTs in the central and northern Cape Basin are $16^\circ\text{--}20^\circ\text{C}$. A -1.5‰ offset of fine fraction $\delta^{18}\text{O}$ values relative to planktonic foraminifera in TN057-21 supports this hypothesis. Temporal changes in sediment focusing were evaluated directly using uranium series radioisotopes. While higher sediment focusing factors would be expected to result in higher alkenone-derived SSTs if sediment advection were the primary control on down-core changes in alkenone-derived SSTs, ^{230}Th -derived focusing factors indicate no such correlation exists. We conclude that alkenone paleotemperature reconstructions from southern Cape Basin drifts reliably record regional SST variations in the Cape Basin. *INDEX TERMS:* 4267 Oceanography: General: Paleooceanography; 1055 Geochemistry: Organic geochemistry; 1040 Geochemistry: Isotopic composition/chemistry; 3022 Marine Geology and Geophysics: Marine sediments—processes and transport; *KEYWORDS:* alkenones, Cape Basin, thorium

Citation: Sachs, J. P., and R. F. Anderson, Fidelity of alkenone paleotemperatures in southern Cape Basin sediment drifts, *Paleoceanography*, 18(4), 1082, doi:10.1029/2002PA000862, 2003.

1. Introduction

[2] Marine climate records capable of resolving millennial-scale events are exceedingly rare, yet essential for understanding the climate system and testing predictive models of climate change in the future. Sediment drifts represent the only open-ocean locations from which such records can be constructed. Fluxes of laterally transported sediment that exceed the vertical flux lead to high accumulation rates at these sites [Bacon, 1984; Bacon and Rosholt, 1982; Suman and Bacon, 1989].

[3] Accurate sea-surface temperature (SST) estimates are fundamental to paleoclimate reconstructions. The ratio of diunsaturated and triunsaturated C_{37} methyl ketones, alkenones, in sediments has been used since the late 1980s to estimate paleotemperatures [Brassell *et al.*, 1986]. The technique is advantageous because alkenones are produced by photoautotrophs that live in surface waters, it can be

applied in locations where carbonate preservation is poor, analytical precision is high and requires gram quantities of sediment, and analysis time is comparable to other paleotemperature estimation techniques. Indeed, where multiple paleotemperature methods have been applied alkenones yield comparable results [Bard, 2001].

[4] Recently this approach has been used to produce high-resolution SST records at sediment drifts in the temperate North and South Atlantic [Lehman *et al.*, 2002; Sachs *et al.*, 2001; Sachs and Lehman, 1999]. Because lateral transport predominates over vertical sedimentation at these locations, careful consideration must be given to the role horizontal advection of sediment may play in shaping the down-core record of paleoclimate proxies that are part of the fine fraction of sediment. Alkenones are likely to be a component of this fraction because they are produced by nanoplankton and because organic carbon in marine sediments is concentrated in silt and clay size fractions [Keil *et al.*, 1994]. It is therefore necessary to demonstrate that down-core variations of alkenone-derived SSTs at sediment drifts reflect local or regional climate and not changes in the

sedimentation regime. Recent work by *Ohkouchi et al.* [2002] demonstrating substantially older radiocarbon ages for alkenones relative to coeval planktonic foraminifera in Bermuda Rise sediment make this scrutiny critical.

[5] Here we present geochemical evidence from three cores in the southern Cape Basin, southeast Atlantic Ocean, demonstrating the fidelity of the alkenone paleotemperature signal there. Our evaluation is based upon reconstructed SSTs in drift and nondrift locations, which are coherent, and on the lack of correlation between sediment focusing factors and SSTs. We attribute early Holocene SSTs that are 4°–6°C warmer than climatological temperatures above the drift site to the transport of alkenones that were produced in warmer waters to the north.

2. Materials and Methods

2.1. Cape Basin Cores TN057-21, TN057-6, and ODP 1089

[6] Geochemical analyses were performed on sediments from three cores from the southern Cape Basin (Table 1 and Figure 1). The longest and most comprehensive data set is from core TN057-21-PC2 (hereafter TN057-21), a 13.9 m core recovered from 4981 m water depth at 41°08'S, 7°49'E in the southern Cape Basin. This site is north of the Agulhas Ridge and south of the contemporary subtropical convergence. Brisk cyclonic currents scour sediment within

Table 1. Sediment Cores From the Cape Basin^a

Core	Latitude	Longitude	Water Depth, m	Sedimentation Rate, cm/kyr
ODP 1089	40°56.18'S	9°53.64'E	4621	16.2
TN057-21-PC2	41°08'S	7°49'E	4981	12.5
TN057-6-PC4	42°54.8'S	8°54'E	3751	3.4

^aSedimentation rates are mean values for the last 110 kyr and are based on the following age models: ODP 1089 [*Hodell et al.*, 2001a], TN057-21 [*Stoner et al.*, 2000], TN057-6 [*Hodell et al.*, 2000].

the basin and deposit it on rapidly accumulating drifts in the southern part [*Tucholke and Embley*, 1984] (Figure 2). Resulting accumulation rates of sediment average 12.5–13.7 cm/kyr [*Ninnemann et al.*, 1999; *Stoner et al.*, 2000], providing excellent resolution in time for an open-ocean location. The ages of the top and bottom of the core are 6 ka and 100–111 ka depending on the timescale used [*Ninnemann et al.*, 1999; *Stoner et al.*, 2000].

[7] ODP Site 1089 was drilled at a sediment drift north of the Agulhas Ridge in 4624 m of water at 40°56.18'S, 9°53.64'E (Figure 1). This position, 176 km ENE of TN057-21, is south of the contemporary subtropical convergence. This drift site had a mean sedimentation rate of 15.7 cm/kyr during the last 600 kyr and 16.2 cm/kyr during the last 110 kyr [*Hodell et al.*, 2001a]. 5 cm³ samples that were 1-cm in thickness (62 years of deposition) were analyzed every 10 cm (620-year resolution) from 14–18 m.

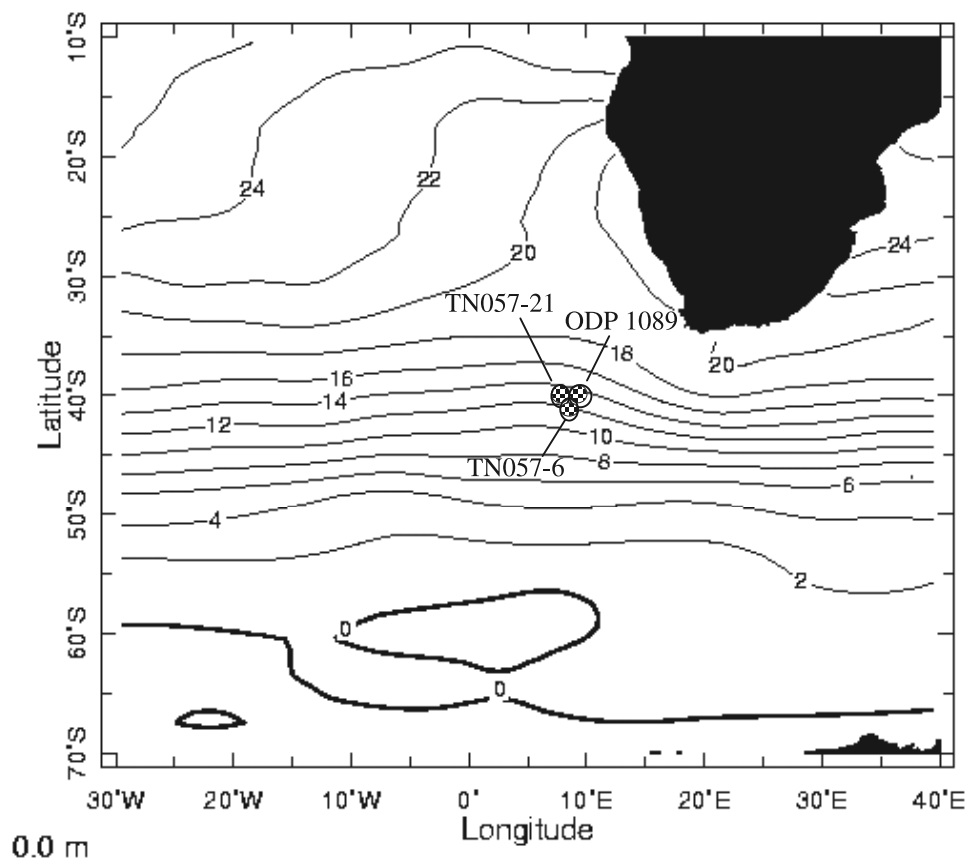


Figure 1. Locations of cores discussed in text overlain on the climatological sea-surface (0 m) temperature field from *Levitus and Boyer* [1994]. Exact positions are provided in Table 1.

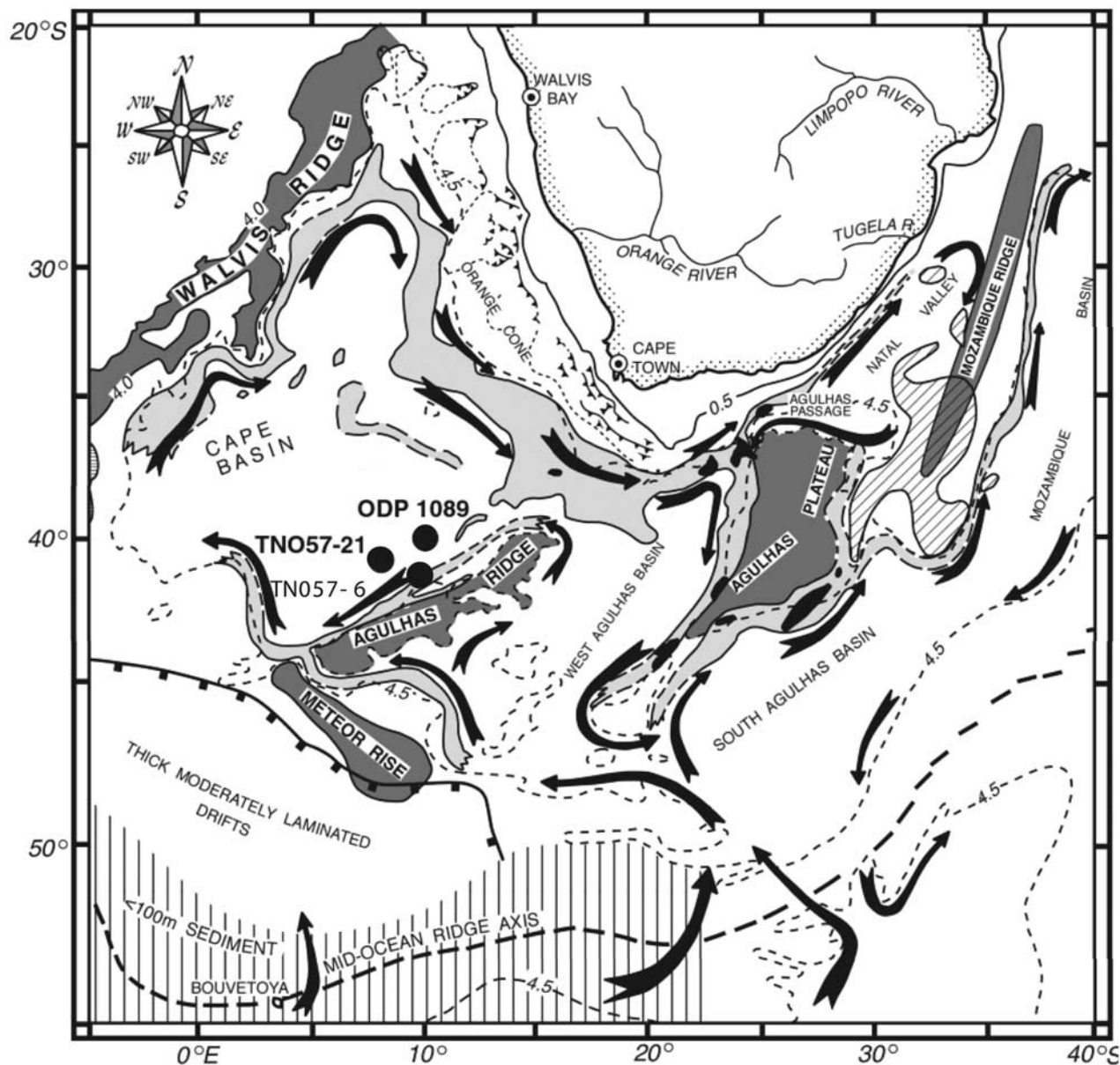


Figure 2. Bathymetric map of the Cape Basin showing the flow of bottom currents and major sedimentation features [Tucholke and Embley, 1984]. Light gray areas are severely eroded. Cores TN057-21 and ODP 1089 were recovered from an extensive drift north of the Agulhas Ridge where winnowed sediment from the Cape Basin to the north and east is focused. Resulting sediment accumulation rates are 12–16 cm/kyr, facilitating climate records with excellent resolution in time. Core TN057-6 was recovered at a shallower depth on the northern slope of the Agulhas Ridge where sediment accumulation rates are closer to 3 cm/kyr.

Sediment samples were removed from the split cores using plastic scoops at the ODP sample repository in Bremen, Germany and placed in a plastic heat-sealed bag, then into a freezer. Sample labels were placed in a separated section of the same bag (using a heat sealer) rather than on the outside of the bags to prevent loss of labels. After shipment to MIT in insulated containers, the sediment was removed from the scoops with solvent-washed stainless steel spatulas and placed into pre-combusted (450°C, >8 hours) glass vials.

[8] Core TN057-6-PC4 (hereafter TN057-6) was recovered from the northern flank of the Agulhas Ridge in 3751 m of water at 42°54.8'S, 8°54'E (Figure 1). This position, 217 km ESE of TN057-21, is south of the contemporary subtropical convergence. The nondrift site had a mean sedimentation rate of 3.0 cm/kyr during the last 424 kyr and 3.4 cm/kyr during the last 110 kyr [Hodell *et al.*, 2000]. The core was sampled and alkenones were analyzed in 1-cm thick intervals (290 years of deposition) every 2-cm

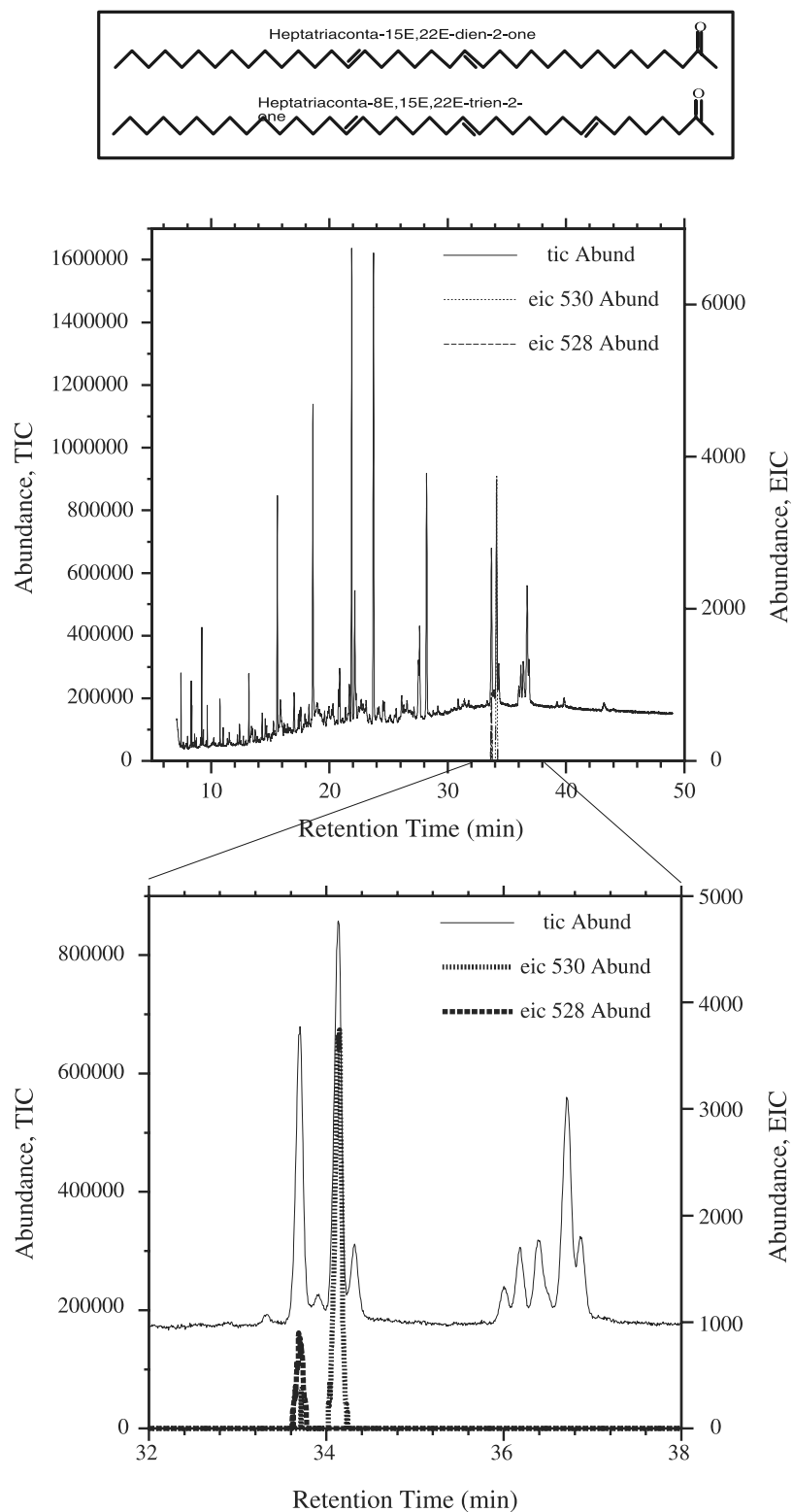


Figure 3. Total ion chromatogram (solid line) of the total lipid extract from 439.5 cm in core TN057-21. Identification of alkenones was performed by GC-MS. Extracted ion chromatograms of the molecular ions of the diunsaturated and triunsaturated alkenone (m/z 530 (dashed line) and 528 (dotted line), respectively) are plotted on the right axis. An expanded view of the alkenone region (32–38 min) of the chromatogram is shown below. The structure of the two alkenones is shown in the box above the chromatograms.

(590-year resolution) in the upper 400 cm of the core using the techniques described below for core TN057-21.

2.2. Alkenone Unsaturation Ratios

[9] The split sediment core was sampled using standard trace-organic clean procedures, and alkenone analyses are as described by *Sachs and Lehman* [1999]. Briefly, samples were stored frozen at -20°C and freeze-dried prior to extraction. After drying, 1–4 g sediment was weighed, and an equivalent quantity of sodium sulfate plus a recovery standard, ethyl triacontanoate, were added. The mixture was loaded into a stainless steel cell and extracted on a Dionex ASE-200 pressurized fluid extractor with methylene chloride. The solvent was evaporated on a Zymark Turbovap II and the lipid extract transferred to a 2 mL autosampler vial. The total lipid extract was redissolved in toluene containing the quantitation standard, *n*-hexatriacontane, and derivatized with bis(trimethylsilyl)-trifluoroacetamide at 60°C for 1 hour. C_{37} methyl ketones (alkenones) were identified by gas chromatography-mass spectrometry (GC-MS) (Figure 3) using an Agilent 6890 GC coupled to an Agilent 5973 MSD. Alkenones were quantified by capillary gas chromatography on an Agilent 6890 GC with a flame ionization detector. All GC and GC-MS was performed with a programmable temperature vaporization (PTV) inlet and a Chrompack CP-Sil-5 60 m \times 0.32 mm i.d. column with 0.25 μm nonpolar phase. GC and GC-MS instrumentation was controlled by Hewlett Packard Chemstation software.

[10] One of three Bermuda Rise sediment standards (BRA, BRB, BRC), prepared from varying mixtures of late Quaternary glacial and interglacial material, was extracted at the beginning and end of each GC sequence (typically containing 50–75 samples). The mean U_{37}^k value and standard deviation of BRA, BRB and BRC samples prepared during the analysis of TN057-21 samples is shown in Table 2. Our analytical precision, the average standard deviation for the three standards, is 0.007 U_{37}^k units, or 0.2°C using the temperature calibration of *Prahl et al.* [1988] (Table 2).

2.3. Alkenone Temperature Calibration

[11] Numerous studies have demonstrated that sedimentary U_{37}^k ($= \text{C}_{37:2}/(\text{C}_{37:2} + \text{C}_{37:3})$, where $\text{C}_{37:2}$ and $\text{C}_{37:3}$ are $n\text{C}_{37}$ methyl ketones with two or three unsaturations, respectively (Figure 3) [*Brassell et al.*, 1986; *Prahl and Wakeham*, 1987]) values record mean annual surface temperatures at 0 m [cf. *Herbert*, 2001; *Müller et al.*, 1998, and references therein]. Global core-top calibrations of the alkenone paleothermometer [*Müller et al.*, 1998] are virtually identical to the original temperature calibration based on cultures of *E. huxleyi*, $\text{U}_{37}^k = 0.034T + 0.039$ [*Prahl et al.*, 1988], and we have adopted that calibration here. Because a number of the 370 sites used in the global calibration of *Müller et al.* [1998] are from the SE Atlantic, and *E. huxley* is the most common coccolithophorid in the SE Atlantic today [*Eynaud et al.*, 1999], that calibration is expected to be accurate for the Cape Basin. Changes in the dominant species of alkenone-producing haptophyte algae through time in the Late Quaternary are not expected to alter the temperature signal obtained from

Table 2. U_{37}^k Values and Associated SSTs for Three Bermuda Rise Sediment Standards Analyzed Repeatedly Throughout This Study^a

	U_{37}^k	1 σ	SST	1 σ	n
Bermuda Rise A	0.73	0.0064	20.24	0.19	141
Bermuda Rise B	0.72	0.0073	20.00	0.22	50
Bermuda Rise C	0.70	0.0072	19.38	0.21	16
Average		0.0070		0.21	

^aThe temperature calibration of *Prahl et al.* [1988] was used to convert U_{37}^k values to SST. Analytical precision is considered to be 0.007 U_{37}^k units, or 0.2°C .

U_{37}^k [*Brassell et al.*, 1986; *Herbert et al.*, 1998; *Müller et al.*, 1997].

2.4. Uranium Series Radioisotopes

2.4.1. Analytical Methods

[12] Uranium and thorium isotopes were measured in aliquots of the 1-cm thick sediment samples from core TN057-21 in which alkenones were measured. Sample spacing varied from 1–4 cm below 380 cm, and 6–35 cm in the upper 380 cm. Measurements were made by isotope dilution inductively coupled plasma mass spectrometry (ICP-MS). A 0.5-g aliquot of dried sediment was dissolved using mixed acids in the presence of ^{229}Th and ^{236}U spikes. After weighing the final solution, an aliquot ($\sim 1.0\%$ by weight) was removed, spiked with ^{230}Th and additional ^{236}U , and diluted with 1% HNO_3 + 1% HF. This solution was analyzed without further processing by ICP-MS to measure concentrations of ^{238}U and ^{232}Th . Uranium and Th in the remainder (99%) of the initial solution were purified by anion exchange chromatography, after which ^{234}U , ^{235}U and ^{230}Th were measured by ICP-MS. Details of the method are presented in the work of *Fleisher and Anderson* [2003].

2.4.2. Unsupported ^{230}Th

[13] Measured concentrations of ^{230}Th in marine sediments consist of three components: that scavenged from seawater; that supported by U contained within lithogenic minerals; and that produced by radioactive decay of authigenic U. Derivation of focusing factors and ^{230}Th -normalized fluxes (see below) make use of only the scavenged component, so measured ^{230}Th concentrations must first be corrected for the presence of the other two components. To make this correction it is generally assumed that the U decay series are in secular equilibrium in lithogenic phases, and that the formation of authigenic U is contemporary with the deposition of the sediments. Accepting those assumptions, unsupported (scavenged from seawater) ^{230}Th ($^{230}\text{Th}_{\text{xs}}$) is calculated from its measured value as:

$$\begin{aligned}
 {}^{230}\text{Th}_{\text{xs}} = & {}^{230}\text{Th}_{\text{meas}} - \left\{ (0.5 \pm 0.1) \cdot {}^{232}\text{Th}_{\text{meas}} \right\} \\
 & - \left\{ \left[{}^{238}\text{U}_{\text{meas}} - (0.5 \pm 0.1) \cdot {}^{232}\text{Th}_{\text{meas}} \right] \right. \\
 & \cdot \left[(1 - e^{-\lambda_{230}t}) + \frac{\lambda_{230}}{\lambda_{230} - \lambda_{234}} \cdot (e^{-\lambda_{234}t} - e^{-\lambda_{230}t}) \right. \\
 & \left. \left. \cdot \left(\left(\frac{{}^{234}\text{U}}{{}^{238}\text{U}} \right)_{\text{init}} - 1 \right) \right] \right\} \quad (1)
 \end{aligned}$$

This equation is applicable when the concentration of each isotope is in units of activity. The first term in curly brackets corrects for ^{230}Th supported by U in lithogenic material, and the second term in curly brackets corrects for ^{230}Th ingrown from authigenic U. To correct for ingrowth from U using the above equations, an estimate of the age of the sediment, t , is required. Here we use stratigraphy derived by independent methods (e.g., $\delta^{18}\text{O}$ or magnetic intensity; see below). Age correction is also generally required in order to correct for the decay of excess ^{230}Th since the formation of the sediment (at time “ t ”). Initial unsupported ^{230}Th ($x_s^{230}\text{Th}(o)$) is then given by:

$$x_s^{230}\text{Th}(o) = {}^{230}\text{Th}_{x_s} \cdot e^{\lambda_{230}t} \quad (2)$$

2.4.3. Lithogenic and Authigenic Uranium

[14] The measured (total) U content of marine sediments consists of authigenic and lithogenic components. The concentration of lithogenic ^{238}U is estimated from the measured concentration of ^{232}Th , which is entirely of lithogenic origin [Brewer *et al.*, 1980], together with an appropriate lithogenic $^{238}\text{U}/^{232}\text{Th}$ ratio. There has never been a formal compilation of lithogenic U/Th ratios in marine sediments. On the basis of our own experience appropriate lithogenic $^{238}\text{U}/^{232}\text{Th}$ ratios (expressed as activity ratios) are 0.6 ± 0.1 for most of the Atlantic Ocean [e.g., Anderson *et al.*, 1994]. However, several studies have found that detrital $^{238}\text{U}/^{232}\text{Th}$ ratios in sediments near Antarctica are systematically lower than elsewhere [Chase *et al.*, 2003]. Here we adopt 0.5 ± 0.1 as the detrital $^{238}\text{U}/^{232}\text{Th}$ activity ratio for the Cape Basin to avoid negative apparent authigenic U concentrations in certain samples. The detrital $^{238}\text{U}/^{232}\text{Th}$ activity ratio adopted here (0.5) is identical to that used for the SW Pacific sector of the Southern Ocean by Chase *et al.* [2003]. Authigenic U is precipitated within chemically reducing marine sediments [Klinkhammer and Palmer, 1991] and it is assumed to have an initial $^{234}\text{U}/^{238}\text{U}$ ratio equivalent to that of U dissolved in seawater (=1.146 [Robinson *et al.*, 2003]). Concentrations of authigenic U are estimated as:

$${}^{238}\text{U}_{\text{auth}} = {}^{238}\text{U}_{\text{meas}} - (0.5 \pm 0.1) \cdot {}^{232}\text{Th}_{\text{meas}} \quad (3)$$

2.4.4. Focusing Factors

[15] Suman and Bacon [1989] introduced the concept of a focusing factor (Ψ) to quantitatively describe the effect of lateral sediment redistribution on the measured accumulation rate of ^{230}Th in sediments. The sediment-focusing factor is defined as:

$$\Psi = \frac{\int_{r_2}^{r_1} [x_s^{230}\text{Th}(o)] \cdot \rho_b \cdot dr}{P_{\text{Th}} \cdot (t_1 - t_2)}, \quad (4)$$

where r_i is the depth at interval i in the core, t_i is the age at depth i , $[x_s^{230}\text{Th}(o)]$ is the decay-corrected concentration of unsupported ^{230}Th in the sediment (equation (2)), P_{Th} is the production rate of ^{230}Th by U decay in the water column above the core site (see below), and ρ_b is the bulk dry density of the sediment.

[16] Ages for the calculation of Ψ were determined by linear interpolation between control points from two published age models for core TN057-21, that from Stoner *et al.* [2000] and that from Ninnemann *et al.* [1999]. The latter was derived from correlation of $\delta^{18}\text{O}$ variations to the SPECMAP stack. Stoner *et al.* [2000] made adjustments to that age model by correlating changes in magnetic intensity of the sediment to changes in cosmogenic nuclide fluxes in Greenland ice cores.

[17] Although a number of algorithms relating in situ density to the CaCO_3 content of sediments have been published, we find that these give unrealistic values for in situ density (in an extreme case, even negative values), at low carbonate contents. Consequently, we have developed our own algorithm based on wet and dry weight measurements from TN057-21 (in situ density (g dry/cc wet) = $0.54849 - 9.7098 \cdot 10^{-5} (\% \text{CaCO}_3) - 1.3115 \cdot 10^{-5} (\% \text{CaCO}_3)^2 + 1.0820 \cdot 10^{-6} (\% \text{CaCO}_3)^3$; $r^2 = 0.874$; $n = 20$). A value of $\Psi > 1$ indicates sediment focusing to the site, whereas $\Psi < 1$ indicates net loss of sediment (winnowing) from the site.

2.4.5. ^{230}Th -Normalized Fluxes

[18] Fluxes corrected for sediment redistribution can be derived by exploiting the known flux of ^{230}Th . The excess ^{230}Th profiling method is based on the assumption that the regionally averaged rain rate of particulate ^{230}Th sinking to the seafloor (F_{Th}) is equivalent to the known rate of ^{230}Th production by ^{234}U decay in the overlying water column (P_{Th}) [Bacon, 1984; Francois *et al.*, 1990]. This assumption has received substantial support from recent studies in which fluxes of particulate ^{230}Th have been evaluated using sediment traps [Scholten *et al.*, 2001; Yu *et al.*, 2001a, 2001b]. Because the residence time of dissolved U in the oceans is long (~ 400 ka; e.g., Henderson [2002]) the production rate of ^{230}Th in seawater has remained virtually constant over the past few 10^5 years. Consequently, the rain rates of any sedimentary component may be deduced as:

$$F_i = \frac{C_i \cdot \beta \cdot z}{x_s^{230}\text{Th}(o)}, \quad (5)$$

where F_i is the flux of a given component “ i ”; C_i is the concentration of “ i ” in a given sediment sample; $\beta \cdot z = P_{\text{Th}}$, where $\beta = 2.6 \cdot 10^{-5} \text{ dpm} \cdot \text{cm}^{-3} \cdot \text{kyr}^{-1}$ and z is depth of water column in cm.

2.5. CaCO_3 and Fine Fraction $\delta^{18}\text{O}$ in TN057-21

[19] Weight percent CaCO_3 determinations were performed on 30–50 mg of oven (50°C) dried sediment using a CO_2 coulometer (UIC Inc. Coulometrics, P/N CM5014) attached to a total inorganic carbon analyzer (UIC Inc. Coulometrics, P/N CM5240) using standard procedures.

[20] Fine fraction $\delta^{18}\text{O}$ analyses were performed on 40–50 μg of oven dried ($< 63 \mu\text{m}$) sediment that had been previously wet-seived at Scripps by Chris Charles. The $\delta^{18}\text{O}$ determination was made with a Micromass Optima stable isotope mass spectrometer with a multiprep sample intro-

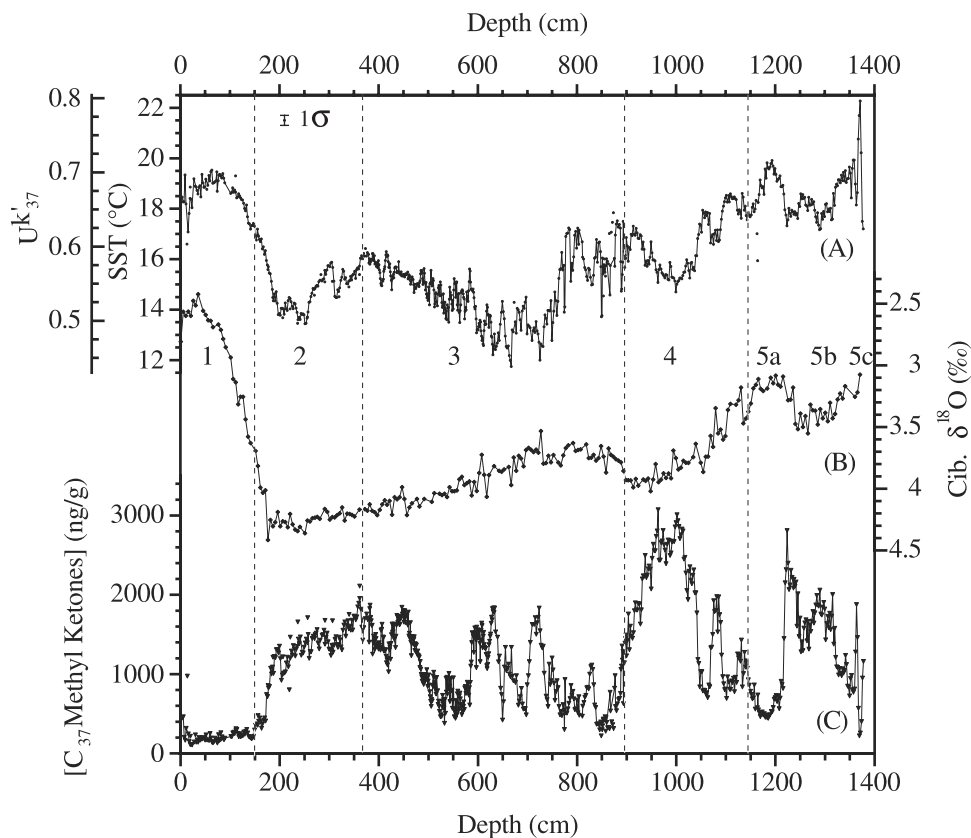


Figure 4. Alkenone data as a function of depth in core TN057-21. (a) U_{37}^k values and SSTs derived from the temperature calibration of *Prahl et al.* [1988]. All replicate analyses are plotted with the line connecting average values. Outliers are also plotted but not connected by the line. (b) $\delta^{18}O$ values from the benthic foraminifera *Cibicidoides* spp. [Ninnemann *et al.*, 1999]. (c) C_{37} methyl ketone (alkenone) concentrations. Marine Isotope Stage (MIS) boundaries [Martinson *et al.*, 1987] are marked by vertical lines and shown in Figure 4b. A one-sigma error bar representing the analytical precision for the U_{37}^k determination in sediments is shown in Figure 4a.

duction system in the laboratory of Richard Fairbanks at Lamont-Doherty Earth Observatory.

3. Results

3.1. Alkenone Concentrations and SST

3.1.1. Core TN057-21

[21] U_{37}^k values in TN057-21-PC2 are between 0.44 to 0.80 and are plotted on a depth scale in Figure 4a. SSTs derived from U_{37}^k values using the *Prahl et al.* [1988] temperature calibration are between 12° and 22°C (Figure 4a). A stratigraphic framework is provided by the oxygen isotope record from benthic foraminifera (*Cibicidoides* spp.) in the same core [Ninnemann *et al.*, 1999] (Figure 4b). Maximum and minimum SSTs occur during MIS 5c and MIS 3, respectively. SSTs of 17.5°–22°C during MIS 5a–c are followed by temperatures of 15°–18.5°C during MIS 4, 12°–17.5°C during MIS 3, 13.5°–18°C during MIS 2, and 17.5°–19.5°C during MIS 1 (Figure 4a). SSTs increase by 6°C, from 13.5° to 19.5°C, during Termination I followed by a gradual cooling trend from 19.5° to 18°C in the early Holocene.

[22] Summed $C_{37:2}$ and $C_{37:3}$ alkenone concentrations in TN057-21 range from 150 to 3200 ng/g (Figure 4c). They are highest in MIS 4 and lowest in MIS 1. There is little or no visual correlation between alkenone concentrations and U_{37}^k -derived SSTs (Figures 4a and 4c).

3.1.2. ODP Site 1089

[23] U_{37}^k -derived SSTs in the studied interval of core ODP 1089 are between 17.5° and 20.5°C (Figure 5d). An oxygen isotope stratigraphy for the core was derived from the planktonic foraminifer *G. bulloides* [Hodell *et al.*, 2001a] (Figure 5a). SSTs reach maxima of 19.5° to 20.5° during MIS 5a and 5c. An extended SST minimum occurs during MIS 5b during which SSTs remain between 17.5° to 18.5°C.

[24] Alkenone concentrations in the studied interval of core ODP 1089 are between 500 and 2900 ng/g (Figure 5c). They are highest (>1500 ng/g) during MIS 5a–b and lowest (<1000 ng/g) during MIS 4 and 5c.

3.1.3. Core TN057-6

[25] U_{37}^k -derived SSTs in the studied interval of core TN057-6 are between 5.5° and 13°C (Figure 6d). A stratigraphy for the core was derived from oxygen isotopes in two species of planktonic foraminifera [Hodell *et al.*, 2000]

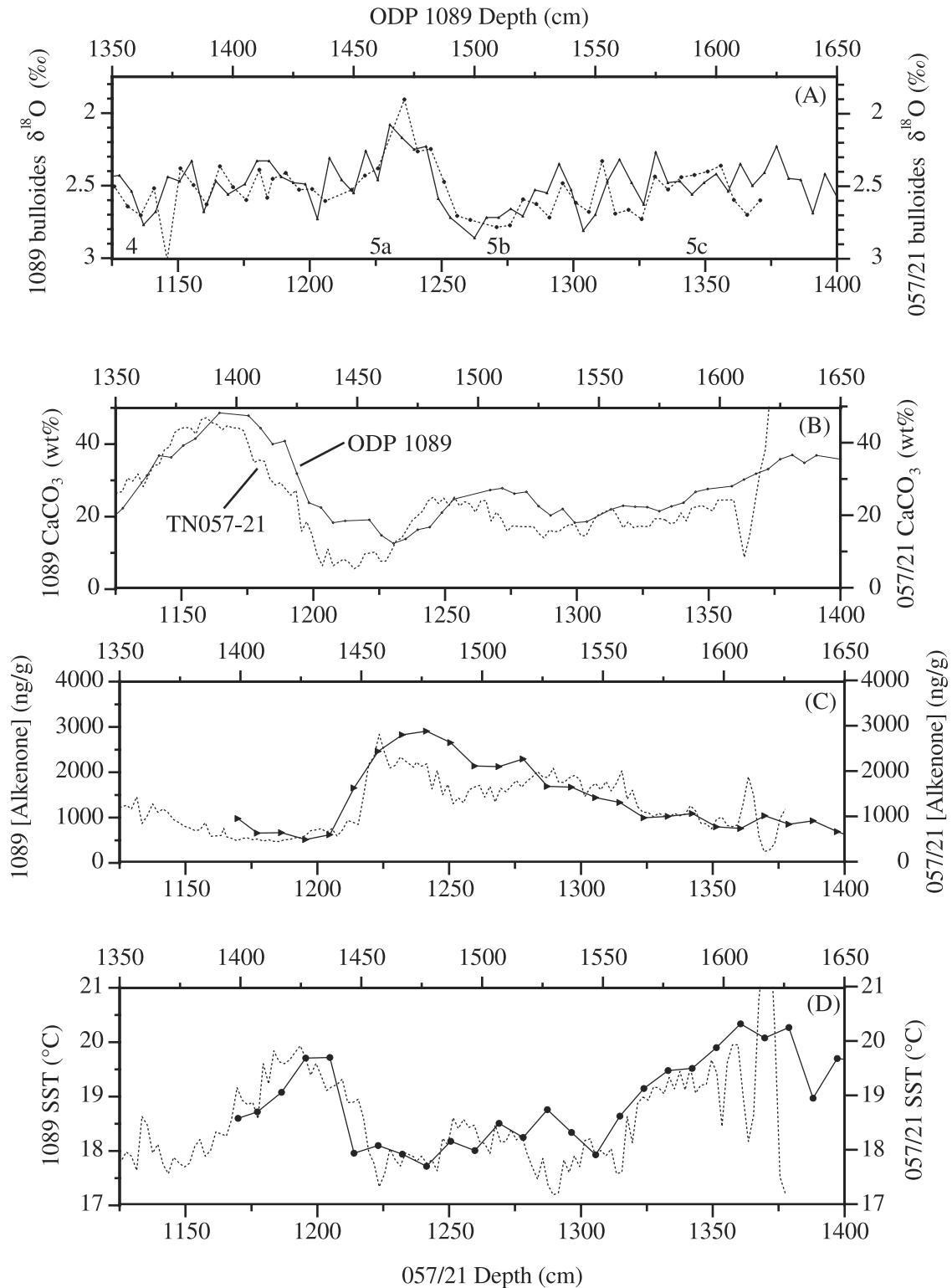


Figure 5. (c) Alkenone concentrations and (d) SSTs at two southern Cape Basin drift sites, TN057-21 (dotted lines) and ODP 1089 (solid lines), are nearly identical during MIS 4–5. The two cores were aligned using $\delta^{18}\text{O}$ values from the planktonic foraminifera, (a) *G. bulloides* and the (b) wt % CaCO_3 values from *Hodell et al.* [2001a].

(Figure 6a). Maximum SSTs of 12°C and above are reached during MIS 5c, 5a, early and late MIS3, and during MIS 1. An extended SST minimum occurs during MIS 3 where temperatures remain between 6°–8°C.

[26] Alkenone concentrations in the studied interval of core TN057-6 are between 10 and 650 ng/g (Figure 6c). They remain below 50 ng/g during MIS 1 and below 100 ng/g during MIS 5a-c. They are higher and more variable during MIS 2–4, with highest sustained values greater than 500 ng/g during MIS 2.

3.2. Calcium Carbonate

[27] Weight percent CaCO₃ varies between 2 and 62% in core TN057-21 (Figure 6b). High carbonate concentrations of 45–60% occur during warm Marine Isotope Stages 1, 3, 5a and 5c, and low carbonate concentrations of 5–20% occur during cool Marine Isotope Stages 2, 4 and 5b. Weight percent CaCO₃ values drop from 62% to 18% during the early Holocene.

[28] Weight percent CaCO₃ values for cores ODP 1089 [Hodell *et al.*, 2001a] and TN057-6 [Hodell *et al.*, 2001b] have been previously published and are shown in Figures 5b and 6b, respectively.

3.3. δ¹⁸O in Bulk < 63 μm Sediment

[29] Oxygen isotope ratios in the fine fraction (<63 μm) of sediment from the upper 1050 cm of TN057-21 are highest (2.25‰) during MIS 4 and 2 (Figure 7b). They are lowest (0.25‰) during the Holocene. They generally follow the temporal trends of benthic (Figure 7c) [Ninnemann *et al.*, 1999] and planktonic (Figure 7b) [Mortyn, 2000] foraminiferal δ¹⁸O. There is an absolute offset of –1.5‰ between the fine fraction and planktonic foraminiferal δ¹⁸O curves (Figure 7b). The deglacial δ¹⁸O change of the <63 μm sediment is 1.75‰, similar to the benthic δ¹⁸O change (Figure 7c) but 0.25‰ larger than the planktonic δ¹⁸O change (Figure 7b). Except for the timing of the start of Termination I, the oxygen isotope records of both fine sediment and planktonic foraminifera share little in common with the alkenone-derived record of SST (Figure 7a).

3.4. Focusing Factors and ²³⁰Th-Normalized Alkenone Fluxes

[30] Focusing factors in TN057-21 range from 2.8 to 54 and average 17 ± 11 (n = 291) using the Stoner *et al.* [2000] age model (Figure 8d, open diamonds) and 14 ± 5.1 (n = 291) using the age model from Ninnemann *et al.* [1999] (Figure 8d, closed diamonds). In addition to a higher average focusing factor the Stoner *et al.* [2000] age model results in larger amplitude and higher frequency variations of the focusing factor than the Ninnemann *et al.* [1999] age model. The close correlation between focusing factors and stratigraphically derived sediment accumulation rates (compare Figures 8d and 8e) results from the relatively uniform initial excess ²³⁰Th in the core. Here we define “stratigraphic accumulation rate” as that derived from an age-depth model to distinguish it from mass accumulation rates derived from excess ²³⁰Th.

[31] High values of the focusing factor in the youngest portion of the record (Figure 8d) may be an artifact of sediment disturbance during coring. The apparent rise in *F*

occurs well into the Holocene, rather than during the glacial termination at a time when many proxy records indicate a reorganization of thermohaline circulation, further supporting our hypothesis that high *F* values reflect disturbance of young sediments.

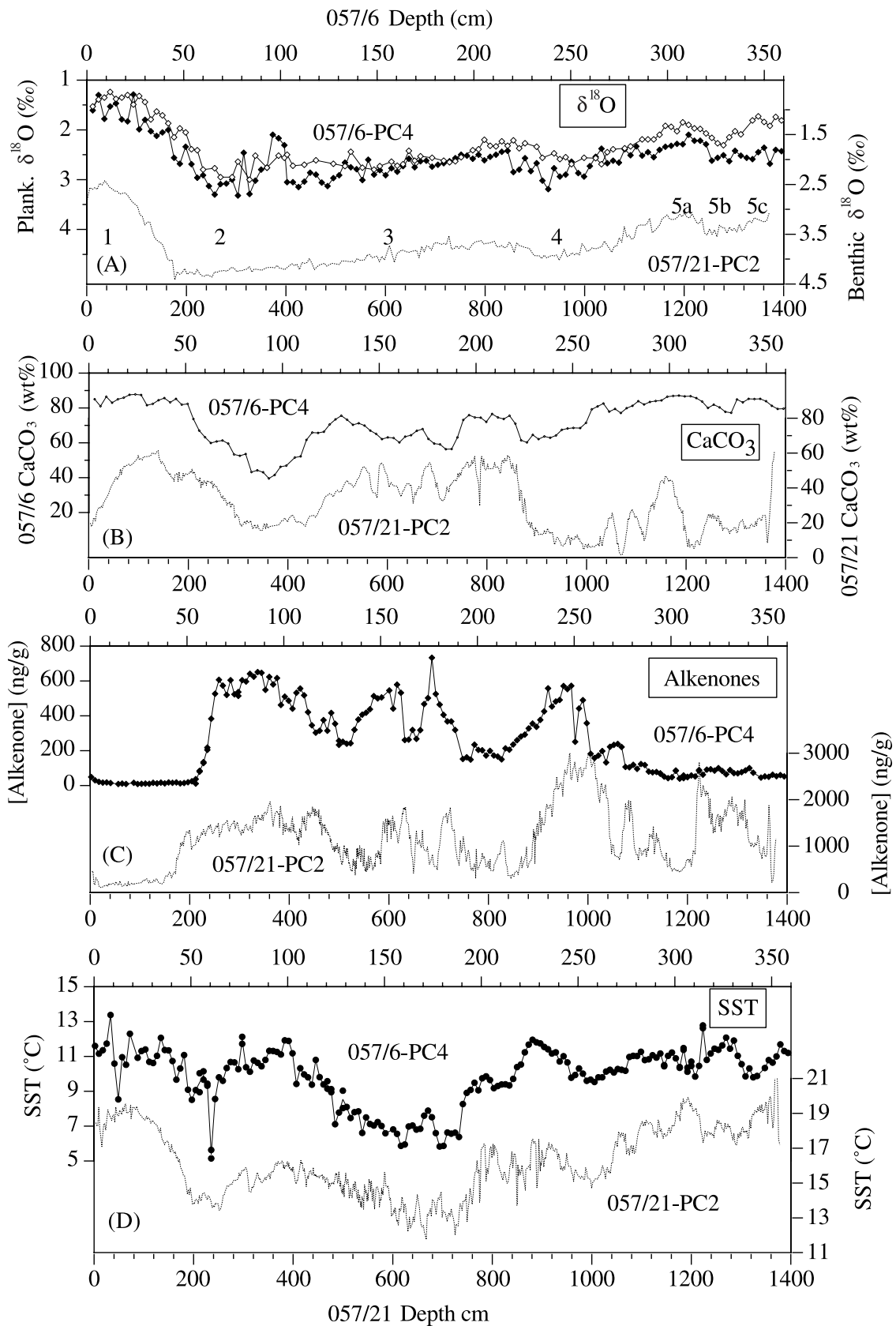
[32] ²³⁰Th-normalized alkenone fluxes, which negate the effect of dilution by other sedimentary components, vary over a 20-fold range between 100 and 2100 ng/cm²/kyr, irrespective of the age model used (Figure 9c). The range and variability of alkenone fluxes is similar to that observed in the record of alkenone concentration (Figure 9b). Consequently, the alkenone concentration record reflects changes in accumulation rate, not changes in dilution by other phases as might be implied by the negative correlation with wt % CaCO₃ (Figure 9a). In addition, no systematic relationship exists between focusing factors and alkenone-derived SSTs (Figure 8a) or alkenone fluxes (Figure 8b).

4. Elevated SSTs in Core TN057-21

[33] Early Holocene SSTs derived from alkenones in core TN057-21 are between 17°–19.5°C (Figure 4a). This compares to climatological SSTs above the core site today of ~13°C (Figure 1) [Levitus and Boyer, 1994]. Because the core-top age is ~6 ka we cannot directly compare our reconstructed Holocene SSTs to the atlas temperature. Evidence that the 4°–6°C SST difference may not be applicable to the late Holocene comes from radiolarian transfer functions in a core 174 km to the east which indicate summer season cooling of 3°–4°C during the latter half of the Holocene [Cortese and Abelmann, 2002]. Nevertheless it is clear that alkenone-derived SSTs in TN057-21 are higher than expected for the latitude of the site (41°S). For example, LGM SSTs of 13.5°C are 0.5°C warmer than climatological SSTs today. Recognizing the wealth of empirical data indicating that alkenone-derived SSTs correspond to mean annual temperatures at 0 m [Herbert, 2001; Müller *et al.*, 1998] we explore alternative explanations for the apparent temperature offset.

[34] We hypothesize that the higher-than-expected SSTs derived from alkenones results from winnowing and focusing of sediment in the Cape Basin to the north and subsequent transport of that sediment to drifts in the south (Figure 2) [Tucholke and Embley, 1984] where core TN057-21 was retrieved. We tentatively attribute a 4°–6°C difference between our reconstructed SSTs and climatological SSTs in the overlying water to the southward transport of alkenones produced in warmer waters to the north. Focusing factors averaging 14–17 during MIS 1-5a (Figure 8c) are evidence for the extensive transport of sediment in the horizontal, relative to the vertical direction at the site of TN057-21. Sediments winnowed from the 30°–40°S latitude band of the Cape Basin (Figure 2) would be expected to yield a regional average alkenone SST of ~18°–19°C (Figure 1).

[35] Another potential source of “warm alkenones” to the southern Cape Basin sediment drifts could be the southwest Indian Ocean via the leakage of Agulhas Current water into the southeast Atlantic. We reason that the magnitude of the Agulhas source is likely to be substantially smaller than the



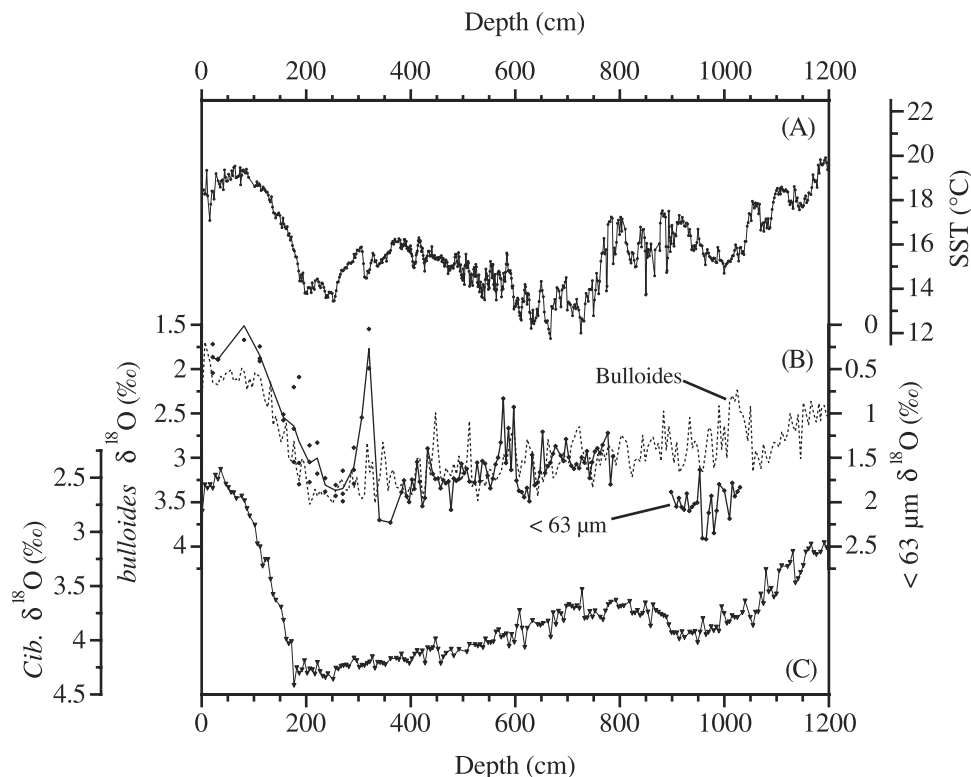


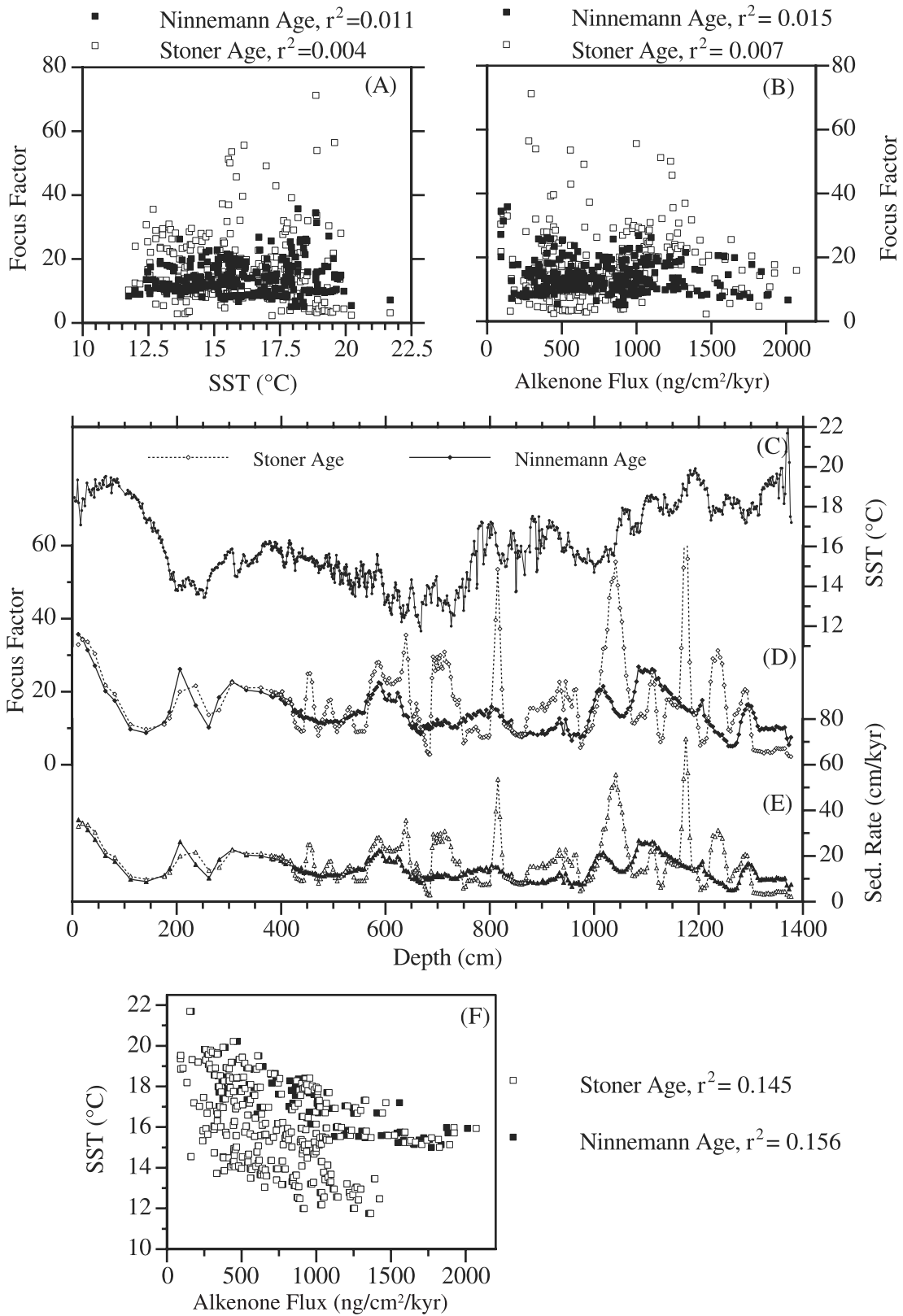
Figure 7. Oxygen isotope ratios in (b) fine-grained (<63 μm) sediment (solid line) and planktonic foraminifera (*G. bulloides*) (dotted line) [Mortyn, 2000] and (c) benthic foraminifera (*Cibicidoides* spp.) [Ninnemann *et al.*, 1999] in TN057-21 are shown with alkenone-derived SSTs (a) in the top 1200 cm of the core. The results of duplicate and triplicate analyses of the fine fraction $\delta^{18}\text{O}$ are plotted with a line connecting the average value at each depth. The three isotope series are plotted with the same y axis range of 2.75‰. For comparison the SST series is plotted on a y scale of 11°C, assuming 4°C of temperature change results in 1‰ of $\delta^{18}\text{O}$ change [Erez and Luz, 1983] and that the entire change in $\delta^{18}\text{O}$ results from temperature. Temporal variations in $\delta^{18}\text{O}$ values of the fine sediment are more similar to both planktonic and benthic $\delta^{18}\text{O}$ series than to the SST series, supporting the notion that horizontal advection of fine sediment on the seafloor is not the first-order cause of downcore variations in SST. Furthermore, the fine fraction $\delta^{18}\text{O}$ series is shifted by -1.5‰ relative to the planktonic $\delta^{18}\text{O}$ series, suggesting an origin for that carbonate in waters 6°C warmer.

central and northern cape Basin source because alkenones from the former would likely have to be transported great distances in the upper ocean. The mass flux of alkenones that can be carried by the handful of Agulhas eddies that enter the Cape Basin each year would seem to be small relative to the mass flux of alkenones produced on the periphery of the northern and central Cape Basin where sediments are winnowed by cyclonic abyssal currents (Figure 2).

[36] The principle benefit of obtaining a regional average SST for the Cape Basin is that local events, such as a

small meridional shift in the position of the subtropical convergence (presently just north of the core site) [Cortese and Abelmann, 2002; Howard and Prell, 1992], may not strongly influence the regional climate signal derived from alkenones at southern Cape Basin drifts. The winnowing and focusing processes also result in high accumulation rates (>10 cm/kyr) and thus excellent resolution in time for an open ocean location. A potential impediment to applying alkenone paleothermometry at this and other drift sites is that sediment advection, rather than surface temperature

Figure 6. (opposite) (d) Alkenone-derived SSTs in core TN057-6, a low accumulation-rate site 217 km ESE of TN057-21, indicate a similar progression of climate during MIS 1-5c. Although sedimentation rates differ by a factor of ~ 4 at the two sites, the stratigraphic relationship between the two cores is firmly established by (a) oxygen isotope records, (b) wt % CaCO_3 , and (c) alkenone concentrations. $\delta^{18}\text{O}$ records from two planktonic foraminifera, *N. pachyderma* (sin.) (open symbols) and *G. bulloides* (closed symbols), in core TN057-6 [Hodell *et al.*, 2000] are compared to the benthic $\delta^{18}\text{O}$ record from *Cibicidoides* spp. (dotted line) in core TN057-21 [Ninnemann *et al.*, 1999] (Figure 6a). All SST estimates in TN057-6, including those from replicate analyses, are plotted with a filled circle in Figure 6d, with the solid line connecting average values and single analyses.



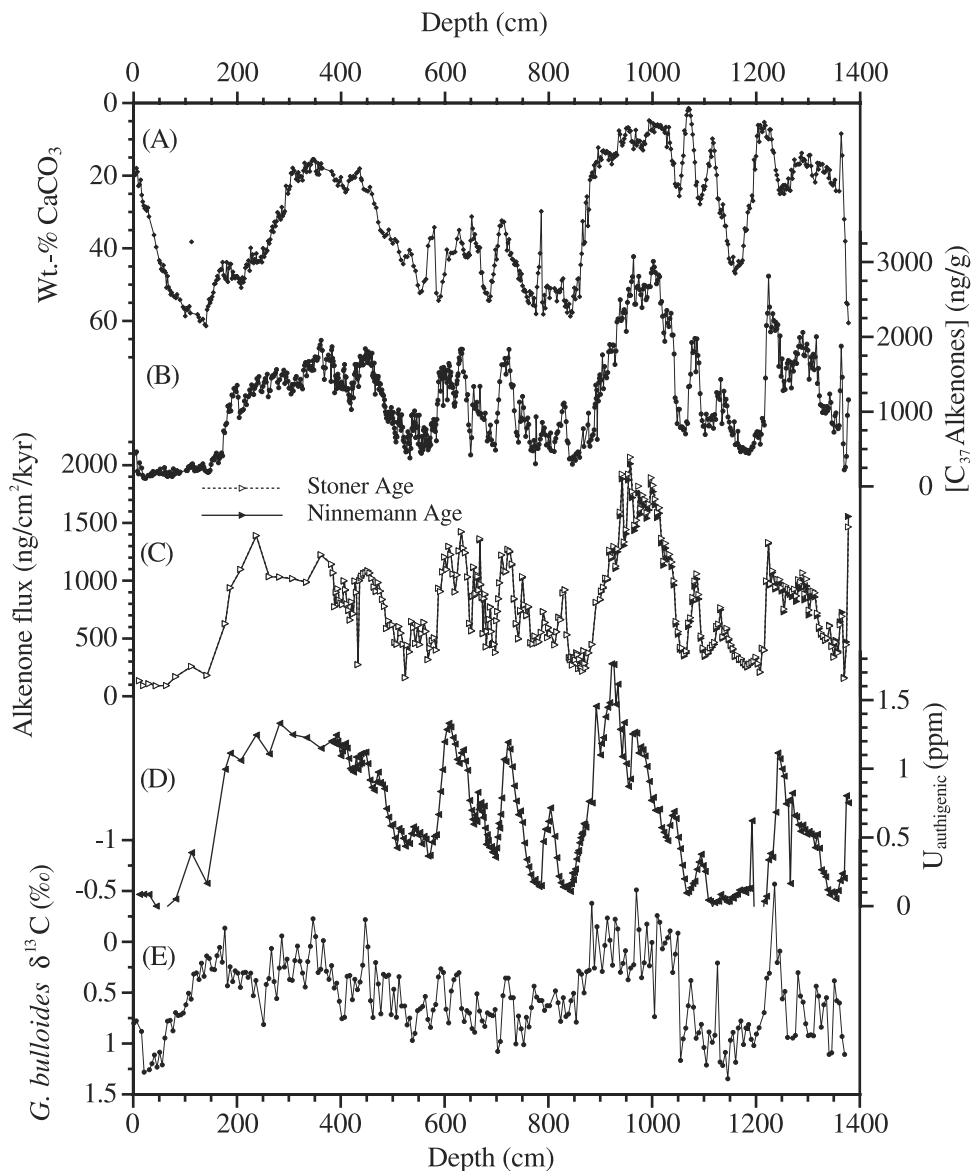


Figure 9. (a) Weight percent CaCO_3 (reversed y axis scale), (b) C_{37} methyl ketone concentration, (c) ^{230}Th -normalized alkenone flux, and (d) authigenic uranium concentration in sediments from core TN057-21. The alkenone flux was calculated using both the age model of *Ninnemann et al.* [1999] (solid line) and that of *Stoner et al.* [2000] (dotted line) to provide decay corrections for ^{230}Th . Concurrent changes in ^{230}Th -normalized alkenone flux (Figure 9c) and alkenone concentration (Figure 9b) indicate that dilution by other sedimentary components did not cause down-core changes in alkenone concentration. Covariation of alkenone fluxes with authigenic uranium concentrations (Figure 9d) suggest that alkenone concentration changes resulted from changes in alkenone production. Concurrent carbon isotopic deletions in the planktonic foraminifera *G. bulloides* [*Ninnemann et al.*, 1999] (Figure 9e) suggest that nutrient enrichment of surface waters may have caused increased alkenone production.

Figure 8. (opposite) Results from uranium series isotope analyses in core TN057-21 indicate that horizontal transport of fine-grained sediment did not the cause observed down-core variations in alkenone-derived temperatures (Figure 4) because sediment focusing is uncorrelated with (a) SST and (b) ^{230}Th -normalized alkenone fluxes. Furthermore, there is little or no correspondence between (c) SST events and (d) focusing events. (e) Sediment accumulation rates calculated from model age-depth relationships are shown. (f) ^{230}Th -normalized alkenone fluxes are shown to be uncorrelated with SSTs, suggesting that alkenone supply is not the primary cause of U_{37}^k SST changes at this drift site. Focusing factors and stratigraphic sedimentation rates were calculated from both the age models of *Ninnemann et al.* [1999] (solid line, closed symbols) and *Stoner et al.* [2000] (dashed line, open symbols).

may drive downcore variations in alkenone unsaturation ratios. This would require that alkenones be associated with the fine (advectible) fraction of sediment, a conservative assumption.

[37] Below we present three lines of evidence that support the fidelity of alkenone paleotemperature records in the southern Cape Basin and refute a predominant role for horizontal sediment advection in driving downcore U_{37}^k changes. This evidence can be summarized as follows: (1) similar alkenone SST trends at nearby nondrift and drift sites; (2) sediment focusing uncorrelated to SST; (3) coherent fine fraction and planktonic foraminiferal $\delta^{18}O$ records.

5. Alkenone Paleotemperatures in Other Cape Basin Cores

[38] Alkenone paleotemperature analyses were performed in two other cores from the southern Cape Basin in order to test the fidelity of the results from TN057-21. ODP Site 1089 was drilled at a drift site 176 km NE of TN057-21 in 4621 m of water (Figure 2). Sedimentation rates during the last 110 kyr averaged 16 cm/kyr. Core TN057-6, located 217 km southeast of TN057-21, was retrieved on the northern flank of the Agulhas Ridge in 3751 m of water (Figure 2). Sedimentation rates there averaged 3.4 cm/kyr during the last 110 kyr, 3.7-fold lower than at the drift site of TN057-21.

5.1. Synchronization of ODP Site 1089 With TN057-21

[39] Reconstructed SSTs in ODP 1089 were compared to those in TN057-21 after the two cores were synchronized in the depth domain using a simple two-tie-point alignment procedure. Planktonic $\delta^{18}O$ records (both *G. bulloides*) (Figure 5a) and wt % $CaCO_3$ (Figure 5b) records from the two cores [Hodell *et al.*, 2001a] were visually aligned to achieve maximum overlap with two tie points: one each at the top and bottom of the studied interval. We aligned 1125 cm in TN057-21 with 1350 cm in ODP 1089, and 1375 cm in TN057-21 with 1625 cm in ODP 1089. This interval spans late MIS 4 through early MIS 5c (Figures 5a and 5b). Carbonate profiles were used to assist with the alignment of the two cores because the $\delta^{18}O$ variations during this interval were relatively small (and/or the signal-to-noise ratio was low).

5.2. Alkenone Paleotemperatures at ODP Site 1089

[40] The resulting correspondence of the alkenone concentration and SST records at the two drift sites is shown in Figures 5c and 5d. (All four parameters, $\delta^{18}O$, wt % $CaCO_3$, alkenone concentration, and SST, are identically scaled in the two cores). Although the resolution of analyses in ODP 1089 is lower, SSTs and the timing and magnitude of their change, as well as the alkenone concentrations are remarkably similar. Coherent and highly reproducible SST changes in cores from two drift sites separated by 176 km supports the fidelity of the alkenone paleotemperature signal in southern Cape Basin drifts. The sediment winnowing and focusing processes in the Cape Basin apparently resulted in alkenone and wt % $CaCO_3$ distributions that remained constant over large spatial scales during MIS4-5c. Thus we speculate that the sediment focusing process in the southern Cape Basin is neither localized nor spatially

heterogeneous, but homogeneously distributes alkenones (and presumably other fine sedimentary components) over a large region of seafloor.

5.3. Synchronization of TN057-6 With TN057-21

[41] Alkenone records from TN057-6 were compared to those in TN057-21 after the two cores were synchronized by matching oxygen isotope stratigraphies as shown in Figure 6a. $\delta^{18}O$ values from two species of planktonic foraminifera in TN057-6, *N. pachyderma* (sin.) and *G. bulloides* [Hodell *et al.*, 2000] were compared to the benthic (*Cibicidoides* spp.) $\delta^{18}O$ record in TN057-21 [Ninnemann *et al.*, 1999]. A continuous, highly resolved benthic $\delta^{18}O$ record was not available from TN057-6 for the interval we studied. Only two tie points were applied: one at the top of both cores, the other tying the bottom of TN057-21 to 350 cm in TN057-6 (Figure 6a). This procedure produces a credible alignment of Marine Oxygen Isotope Stages 1–5 in the two cores. It also results in a reasonable alignment of features in the wt % $CaCO_3$ (Figure 6b) and alkenone concentration (Figure 6c) profiles at the drift and nondrift sites.

[42] We opted for a comparison of $\delta^{18}O$ series in the depth domain of the two cores, rather than using published timescales derived by correlating $\delta^{18}O$ records to various reference time series [Hodell *et al.*, 2000; Mortyn, 2000; Ninnemann *et al.*, 1999; Stoner *et al.*, 2000; D. Hodell, personal communication, 2002], because it is more direct, objective and requires fewer assumptions. That is, rather than compare the alkenone data from TN057-6 and TN057-21 on timescales derived from separate visual correlations of $\delta^{18}O$ data to either the same or different reference time series, we chose to visually correlate the two $\delta^{18}O$ series directly. In addition, at least three published age models exist for TN057-21 [Mortyn, 2000; Ninnemann *et al.*, 1999; Stoner *et al.*, 2000] and two for TN057-6 (one published in the work of Hodell *et al.* [2000], the other unpublished (C. Charles and D. Hodell, personal communication, 2002)), requiring a somewhat arbitrary choice of one over another.

[43] As discussed in detail in section 8, we attribute the breakdown of the visual correlation between alkenone concentration profiles in the two cores during MIS 5a-c (e.g., depths greater than ~275 cm in TN057-6 and ~1100 cm in TN057-21) (Figure 6c) to dilution of alkenones by $CaCO_3$ in TN057-6 (Figure 6b).

[44] The observed lead of planktonic $\delta^{18}O$ values in TN057-6 relative to benthic $\delta^{18}O$ values in TN057-21 at the beginning of Termination I may indicate that the tie point at the core tops may not be valid or that sedimentation rate changes during MIS 2 and 3 (MIS 4-5c being better constrained by isotopic changes) alter the stratigraphic relationship between the two cores. Another possibility is that both of the former contribute to the apparent phase difference of the $\delta^{18}O$ series at the start of Termination I. Nevertheless, the offset in the two cores is consistent with a (~2 kyr) lead in planktonic relative to benthic $\delta^{18}O$ values in Cape Basin cores TN057-21 (Figures 7b and 7c) [Mortyn, 2000; Ninnemann *et al.*, 1999], ODP 1089 [Hodell *et al.*, 2001a], TN057-6 [Hodell *et al.*, 2000] (and many other cores [cf. Lea, 2001]) at that time. Whether real or an

artifact of our synchronization, the offset of the alkenone concentration decline associated with Termination I in TN057-6 relative to that in TN057-21 (Figure 6b) suggests that the lead of planktonic relative to benthic $\delta^{18}\text{O}$ in the two cores is overestimated. Whatever the cause of the offset, we opt for the simple two-tie-point synchronization because it requires the fewest assumptions and is adequate for evaluating the two long alkenone records.

5.4. Alkenone Paleotemperatures in TN057-6

[45] SST changes reconstructed from alkenones in core TN057-6 are coherent with those from the drift site (TN057-21) throughout the ~ 100 kyr record (Figure 6d). If the downcore SST signal at the drift site was strongly influenced by changes in sediment focusing we would not expect to see a similar pattern of SST change at a nearby nondrift site with sedimentation rates ~ 4 -fold lower. Furthermore, alkenone-derived SSTs in the Holocene section of TN057-6 (12° – 13°C) are very similar to climatological SSTs above the site today (Figure 1) [Levitus and Boyer, 1994] suggesting that alkenones are faithful recorders of SST there. A near-constant offset of $+6^\circ\text{C}$, less than 15% of which can be ascribed to climatological differences between the two sites (in the contemporary Southern Ocean), supports our notion that the reconstructed SSTs from TN057-21 and ODP 1089 are elevated by the winnowing and transport of alkenones produced in warmer waters to the north. Most importantly, coherent SST changes in TN057-21 and TN057-6 during MIS 1-5 strongly support the fidelity and regional representativeness of the alkenone paleotemperature signal in the southern Cape Basin drift site of TN057-21 (Figure 6d).

6. Sediment Focusing and ^{230}Th -Normalized Alkenone Fluxes

[46] Sediment accumulating at drift sites in the southern Cape Basin may be advected long distances and is likely to contain alkenones. Indeed, we hypothesize that the alkenone paleotemperatures from cores TN057-21 and ODP 1089 are $\sim 6^\circ\text{C}$ warmer than those in nearby core TN057-6 because the two drift cores receive alkenones (and sediment) produced in warmer waters to the north. In the previous section we presented evidence that down-core changes in sediment advection were not the first-order cause of changes in alkenone paleotemperatures at those drifts based upon coherent alkenone-derived SSTs at a nearby low-accumulation rate site (TN057-6). Here we use ^{230}Th -based estimates of sediment focusing in TN057-21 to investigate directly whether changes in sediment advection were associated with changes in alkenone-derived SSTs.

[47] The focusing factor (Ψ) is defined as the decay-corrected accumulation rate of unsupported ^{230}Th (dpm/cm²/kyr) (i.e., the thorium that did not derive from uranium decay in the sediment) divided by the production rate of ^{230}Th by U decay in the overlying water column [Bacon, 1984; Francois and Bacon, 1991; Suman and Bacon, 1989]. Because thorium is extremely particle reactive Ψ can be used to determine the factor by which the horizontally advected mass flux of sediment exceeds the vertical flux (see section 2.4.4). If changes in SST in the drift cores were

caused by changes in the intensity of horizontal advection of alkenones produced in warmer waters to the north then we expect that increases in Ψ would be associated with increases in alkenone-derived SSTs. This expected relationship is not observed in the data (Figures 8a, 8c, and 8d).

[48] Because focusing factors are age model-dependent, there is a potential concern that the lack of correlation between focusing factor and alkenone-derived SST results from errors in the age model used to derive focusing factors. Therefore focusing factors and sediment accumulation rates were calculated using two different age models for core TN057-21 (see section 2.4.4) (Figures 8d and 8e). Irrespective of the age model used there is no dependence of alkenone-derived SSTs on focusing factors during MIS 1-5c (Figures 8a, 8c, and 8d). Thus, although sediment focusing elevated U_{37}^k values above those expected for the local sinking flux, it did not cause the variations we observe in down-core alkenone SSTs.

[49] Even in the absence of changes in sediment focusing or regional Cape Basin SSTs the potential exists for changes in the rate of alkenone production in different regions of the Cape Basin to cause changes in U_{37}^k SSTs recorded in southern Cape Basin drifts. For instance, if an increase in alkenone production occurred in the central or northern Cape Basin, but was not associated with a change in alkenone production in the southern part or by any change in Cape Basin SSTs or sediment focusing, U_{37}^k SSTs might still be expected to increase in TN057-21. While we cannot discern the origin of alkenones in TN057-21 we can test the possibility that alkenone-derived SSTs in the core reflect changes in alkenone supply. A plot of ^{230}Th -normalized alkenone fluxes versus SST indicates no correlation between the two parameters ($r^2 = 0.15$ or 0.16 with the Stoner *et al.* [2000] and Ninnemann *et al.* [1999] age models, respectively) (Figure 8f). We conclude therefore that changes in alkenone supply to this southern Cape Basin drift were not the primary cause of downcore changes in alkenone-derived SSTs. Nevertheless, based on this analysis alone, we cannot rule out a role for changes in the relative contribution of alkenones from different regions within the Cape Basin. The close covariation in TN057-21 and TN057-6 of both SSTs and alkenone concentrations, however, argue strongly against this mechanism. (See section 8 for a further discussion of alkenone production changes in the Cape Basin.)

7. Fine Fraction $\delta^{18}\text{O}$

[50] Oxygen isotope ratios in the fine ($< 63 \mu\text{m}$) fraction of sediment covary with planktonic foraminiferal $\delta^{18}\text{O}$ values [Mortyn, 2000], with an offset of -1.5‰ (Figure 7b). Because fine fraction sediment [Berger *et al.*, 1978] and mixed calcareous nannofossil [Goodney *et al.*, 1980] $\delta^{18}\text{O}$ values closely track surface-most dwelling foraminiferal $\delta^{18}\text{O}$ values they may be useful as an oxygen isotopic surrogate for the surface waters where fine fraction carbonate originates. If alkenones are associated with the fine fraction of sediment, a conservative assumption, then the fine fraction $\delta^{18}\text{O}$ may have been imparted in the same water in which the alkenones were produced. We thus

interpret the 1.5‰ isotopic depletion of fine fraction carbonate relative to *G. bulloides* $\delta^{18}\text{O}$ in Figure 7b as indicative of warmer or fresher surface waters in the region where the alkenones and fine fraction carbonate were produced. Culture studies indicating that coccoliths display the temperature-dependent fractionation expected for equilibrium calcite [Dudley *et al.*, 1986] imply that the fine fraction carbonate was produced in water $\sim 6^\circ\text{C}$ warmer than the *G. bulloides*, assuming the entire 1.5‰ offset was due to temperature. This temperature difference is consistent with the difference between mean early Holocene SSTs and atlas temperatures and the SST offset between the drift (TN057-21 and ODP 1089) and nondrift (TN057-6) cores.

[51] Another possible source of ^{18}O -depleted carbonate in sediment $<63\ \mu\text{m}$ is surface water over the site of TN057-21. According to Mortyn [2000] the predicted difference in calcite $\delta^{18}\text{O}$ between zero and 100 m water depth at that location is on the order of 1.5‰. Coccoliths and juvenile foraminifera living at the surface might be depleted in ^{18}O by the amount we observe relative to *G. bulloides*. However, we reason that with the majority of sediment mass accumulation resulting from lateral advection (focusing factors average 14–17) of distally produced material, including CaCO_3 , it is unlikely that the local flux of fine-fraction carbonate would dominate the fine-fraction carbonate in the drift sediment. Nevertheless, it is plausible that any fine-grained CaCO_3 produced in the overlying surface water would be depleted in ^{18}O relative to *G. bulloides* in the drift sediment.

[52] Closer similarity of the fine fraction and *bulloides* $\delta^{18}\text{O}$ records to the benthic $\delta^{18}\text{O}$ series (Figure 7b) as compared to the SST series (Figure 7a) implies the influence of factors other than temperature. In addition to variations in ocean $\delta^{18}\text{O}$ caused by ice volume changes we hypothesize that substantial salinity changes occurred in either or both the surface waters overlying TN057-21 and those waters in which the $<63\ \mu\text{m}$ - CaCO_3 was produced. Shifting positions of the subtropical convergence (STC) [Cortese and Abelmann, 2002; Howard and Prell, 1992], with saltier water to the north and fresher water to the south, may have caused these changes.

8. Alkenone Production Changes in the Cape Basin

[53] Alkenone concentration profiles in the drift (TN057-21) and nondrift (TN057-6) cores share many of the same features (Figure 6c), suggesting widespread alkenone production changes in the Cape Basin. In addition to the ~ 10 -fold decline in concentration associated with Termination I, there is a broad concentration maximum spanning MIS 2 and the latter part of MIS 3 in both cores. Furthermore, three concentration minima (at 500–575 cm, 650–700 cm, and 750–900 cm in TN057-21) and three maxima (at 600–650 cm, 700–750 cm, and 900–1050 cm in TN057-21) occur during MIS 3–4 in both cores (Figure 6c). Although the absolute concentrations of alkenones is ~ 3 -fold lower in TN057-6 than in TN057-21 we hypothesize that concurrent relative changes in concentration reflect the same physical and/or biological processes at both locations.

[54] Of the three processes that contribute to alkenone concentration changes in sediments we surmise that production predominates over preservation and dilution during most of the last glacial period at these Cape Basin sites. While it is tempting to interpret the inverse variation between wt % CaCO_3 and alkenone concentrations in TN057-21 (Figures 9a and 9b) as the result of dilution of alkenones by carbonate, ^{230}Th -normalized alkenone fluxes in TN057-21 (Figure 9c) remove this effect and exhibit nearly identical features as the ~ 100 kyr alkenone concentration record (Figure 9b). Additional evidence against dilution controlling alkenone concentrations is the decoupling of carbonate and alkenone concentration profiles in the Holocene section of TN057-21 (Figures 9a and 9b). During that time wt % CaCO_3 decreased from 60% to 20% while alkenone concentrations and fluxes remained low and quite constant (Figures 9b and 9c).

[55] The similarity of the alkenone concentration profiles in TN057-21 and TN057-6 (Figure 6c) argues for a similar control of alkenone concentrations by production rate changes at the nondrift site during MIS 1-5a. However, we tentatively attribute the breakdown of the visual correlation between alkenone concentration profiles in the two cores during MIS 5a-c (i.e., depths greater than ~ 275 cm in TN057-6 and ~ 1100 cm in TN057-21) to dilution of alkenones by CaCO_3 in TN057-6 (Figure 6c). Carbonate preservation is substantially better at the shallower depth of TN057-6 than at the deeper drift site, especially during MIS 5 when wt % CaCO_3 values at the shallower site vary between 80% and 90% versus 10% to 35% at the deeper site [Hodell *et al.*, 2001b]. Confirmation of this hypothesis must await the results of planned ^{230}Th analyses in TN057-6.

[56] While dilution can be ruled out as an important control on alkenone concentration changes in TN057-21 with ^{230}Th -normalized flux determinations, authigenic uranium (U_{auth}) concentrations can be used to distinguish between the importance of alkenone production and preservation in dictating alkenone concentrations. U_{auth} concentrations in TN057-21 (Figure 9d) covary with alkenone fluxes (Figure 9c) suggesting that the total flux of organic matter to the seafloor (of which alkenones were presumably a minor component) varied with the flux of alkenones. While the U_{auth} changes may reflect changes in bottom-water O_2 concentration (which can influence alkenone preservation [Gong and Hollander, 1999; Hoefs *et al.*, 1998; Prahl *et al.*, 1989; Teece *et al.*, 1998]) and bottom-water O_2 concentrations may have changed independently of changes in organic carbon fluxes, we believe this mechanism is less compelling based upon the differing modern hydrography of the two sites. The deeper drift site is bathed by almost pure Circumpolar Deep Water (CDW). The shallower nondrift site is located near the center of the mixing zone between CDW and North Atlantic Deep Water (NADW) [Hodell *et al.*, 2001b]. Changes in alkenone concentration are so well correlated between the two sites that a preservation mechanism would require substantial simultaneous changes in the oxygen concentration of both CDW and NADW, which seems unlikely. Furthermore, Chase *et al.* [2001] concluded that the pattern of authigenic U deposition in South Atlantic sediments during the LGM is

more consistent with an origin related to regional changes in primary production and carbon fluxes to the seafloor rather than with changes in deep-water oxygen concentration [Chase *et al.*, 2001].

[57] Although lower absolute concentrations of alkenones in TN057-6 relative to TN057-21 may be due to poorer preservation resulting from lower sedimentation rates [c.f. Henrichs and Reeburgh, 1987], it is unlikely that simultaneous changes in sedimentation rate resulted in similar alkenone concentration profiles during MIS 1-5a (Figure 6c) given the different sedimentation regimes at the two sites. We also note that there is no correlation between ^{230}Th -normalized alkenone fluxes and focusing factors in TN057-21 ($r^2 = 0.007$ or 0.015 with the Stoner *et al.* [2000] and Ninnemann *et al.* [1999] age models, respectively) (Figure 8b). This indicates that the processes controlling alkenone accumulation at this southern Cape Basin drift site are independent of those controlling sediment accumulation (i.e., focusing).

[58] Consistent with our hypothesis that production rate changes caused down-core variations of alkenone concentrations in TN057-21 is their close covariation with *G. bulloides* $\delta^{13}\text{C}$ values published previously by Ninnemann *et al.* [1999] (Figure 9e). Planktonic $\delta^{13}\text{C}$ values are thought to reflect nutrient concentrations, among other factors [Ninnemann and Charles, 1997; Spero and Lea, 2002]. Except during the last glacial termination, *bulloides* $\delta^{13}\text{C}$ values are low when alkenone concentrations are high (Figures 9b and 9e). Higher nutrient concentrations in surface waters overlying TN057-21 would be consistent with elevated alkenone production in the Cape Basin at those times.

[59] We thus conclude that changes in alkenone production, rather than preservation or dilution, caused the simultaneous changes in alkenone concentration observed during MIS 1-5a in TN057-6 and TN057-21.

9. Conclusions

[60] Taken together, there is compelling evidence indicating that paleotemperatures derived from alkenones in core TN057-21 in particular, and southern Cape Basin drifts in general, are reliable, regional temperatures for the Cape Basin. This is the simplest, most direct interpretation of coherent U_{37}^k -derived SSTs in cores from two drift sites (TN057-21 and ODP 1089) and a nearby nondrift site (TN057-6). The fidelity of alkenone SSTs in TN057-21 is further supported by their lack of correlation with sediment focusing factors and by coherent $\delta^{18}\text{O}$ changes in fine fraction sediment and planktonic foraminifera.

[61] SSTs in the early Holocene section of TN057-21 that are 4° – 6°C warmer than expected based on atlas temperatures are best explained by advection of alkenones that were produced in warmer waters to the north. A -1.5‰ offset of fine fraction $\delta^{18}\text{O}$ values relative to planktonic foraminiferal $\delta^{18}\text{O}$ values supports this notion. Nearly identical SSTs and alkenone concentrations in ODP 1089, drilled 176 km to the northeast, indicate that the winnowing and focusing processes resulted in a homogenous distribution of alkenones over large spatial scales in the southern

Cape Basin. Early Holocene SSTs in TN057-6 that are similar to atlas SSTs indicate that alkenones at this nearby nondrift location faithfully record overlying surface temperatures.

[62] Three features of the SST records are of particular note. The first is the 5° – 6°C of cooling in the early part of MIS 3 (Figure 6d). While a cooling trend in the Cape Basin at this time may coincide with cooling at the end of either interstadial 14 in Greenland or warm event A3 in Antarctica [Blunier and Brook, 2001] the magnitude of the Cape Basin event is very large relative to other cooling episodes in that record. The second and third features of note in both records, which were previously reported for core TN057-21 [Sachs *et al.*, 2001], are a 4° – 5°C warming followed by a 2.5° – 3°C cooling during the latter part of MIS 3 and MIS 2. A similar temperature progression was inferred from measurements of the deuterium excess in central east Antarctic ice cores [Jouzel *et al.*, 1982; Vimeux *et al.*, 1999] for moisture source regions in temperate southern latitudes [Armengaud *et al.*, 1998; Koster *et al.*, 1992]. Yet the SST features are noteworthy because they occur during a period of increasing global ice volume and cooling in Antarctica and Greenland. As proposed by Sachs *et al.* [2001], potential causes of Cape Basin warming during late MIS 3 include reduced NADW production, enhanced Ekman heat transport from tropical- to middle-latitude surface waters, a poleward shift of the westerlies, and increased leakage of Agulhas Current water into the Atlantic.

[63] Synchronous alkenone concentration variations in the three cores are most likely the result of widespread changes in alkenone production rates in the Cape Basin. Covariation of ^{230}Th -normalized alkenone fluxes with alkenone concentrations in TN057-21 rules out dilution as an important control on the latter. While concurrent changes in authigenic uranium concentrations and alkenone fluxes may be consistent with both preservation and production being important determinants of alkenone concentration, alkenone production rate changes are probably the more important process. Coherent alkenone concentration changes in TN057-6 and TN057-21 argue against the importance of preservation because the sedimentation rates and bottom water chemistry at the two sites are markedly different.

[64] Sediment drifts remain the only locations where the marine record of rapid climate change in the Quaternary can be reconstructed. Careful evaluation of multiple geochemical parameters in multiple cores is necessary to evaluate the fidelity of climate proxies that are associated with the fine fraction of sediment at drift sites. We have demonstrated that drift deposits in the southern Cape Basin yield faithful paleotemperature records derived from alkenones.

[65] **Acknowledgments.** Alkenone analyses in core TN057-6 were performed almost entirely by Maria Schriver as part of an MIT UROP project in the summer of 2002. We thank Ying Chang for assistance analyzing alkenones, Marty Fleisher for assistance measuring uranium series isotopes, Martha Bryan for assistance sampling the TN057 cores, and Rick Fairbanks and Martha Bryan for assistance measuring CaCO_3 and fine fraction $\delta^{18}\text{O}$. The Ocean Drilling Program provided sediment samples from Site 1089. Useful discussions with John Hayes, Jerry McManus, and Tom Koutavas contributed to this manuscript. Chris Charles supplied sediment fine fractions from TN057-21-PC2. This

research was supported by the Jephtha H. and Emily V. Wade Foundation and a Henry L. and Grace Doherty Professorship to J.P.S., and by a grants/cooperative agreement from the National Oceanic and Atmospheric

Administration; NOAA Award NA77RJ0453. The views expressed herein are those of the authors and do not necessarily reflect the views of NOAA or any of its subagencies.

References

- Anderson, R. F., M. Q. Fleisher, P. E. Biscaye, N. Kumar, B. Ditrach, P. Kubik, and M. Suter, Anomalous boundary scavenging in the Middle Atlantic Bight—Evidence from ^{230}Th , ^{231}Pa , ^{10}Be and ^{210}Pb , *Deep Sea Res., Part II*, 41(2–3), 537–561, 1994.
- Armengaud, A., R. D. Koster, J. Jouzel, and P. Ciais, Deuterium excess in Greenland snow: Analysis with simple and complex models, *J. Geophys. Res.*, 103, 8947–8953, 1998.
- Bacon, M. P., Glacial to interglacial changes in carbonate and clay sedimentation in the Atlantic Ocean estimated from ^{230}Th measurements, *Chem. Geol.*, 2, 97–111, 1984.
- Bacon, M. P., and J. N. Rosholt, Accumulation rates of Th-230, Pa-231, and some transition metals on the Bermuda Rise, *Geochim. Cosmochim. Acta*, 46, 651–666, 1982.
- Bard, E., Comparison of alkenone estimates with other paleotemperature proxies, *Geochim. Geophys. Geosys.*, 2, Paper number 2000GC000050, 2001.
- Berger, W. H., J. S. Killingley, and E. Vincent, Stable isotopes in deep-sea carbonates: Box core ERDC-92, west equatorial Pacific, *Oceanol. Acta*, 1, 203–216, 1978.
- Blunier, T., and E. J. Brook, Timing of millennial-scale climate change in Antarctica and Greenland during the last glacial period, *Science*, 291, 109–112, 2001.
- Brassell, S. C., G. Eglinton, I. T. Marlowe, U. Pflaumann, and M. Sarnthein, Molecular stratigraphy: A new tool for climatic assessment, *Nature*, 320, 129–133, 1986.
- Brewer, P. G., Y. Nozaki, D. W. Spencer, and A. P. Fleer, Sediment trap experiments in the deep North Atlantic: Isotopic and elemental fluxes, *J. Mar. Res.*, 38, 703–728, 1980.
- Chase, Z., R. F. Anderson, and M. Q. Fleisher, Evidence from authigenic uranium for increased productivity of the glacial Subantarctic Ocean, *Paleoceanography*, 16, 468–478, 2001.
- Chase, Z., R. F. Anderson, M. Q. Fleisher, and P. Kubik, Accumulation of biogenic and lithogenic material in the Pacific sector of the Southern Ocean during the past 30,000 years, *Deep Sea Res., Part II*, 50, 799–832, 2003.
- Cortese, G., and A. Abelman, Radiolarian-based paleotemperatures during the last 160 kyr at ODP Site 1089 (Southern Ocean, Atlantic sector), *Palaeogeogr. Palaeoclimatol. Palaeoecol.*, 182, 259–286, 2002.
- Dudley, W. C., P. Blackwelder, L. Brand, and J.-C. Duplessy, Stable isotopic composition of coccoliths, *Mar. Micropaleontol.*, 10, 1–8, 1986.
- Erez, J., and B. Luz, Experimental paleotemperature equation for planktonic foraminifera, *Geochim. Cosmochim. Acta*, 47, 1025–1031, 1983.
- Eynaud, F., J. Giraudeau, J.-J. Pichon, and C. J. Pudsey, Sea-surface distribution of coccolithophores, diatoms, silicoflagellates and dinoflagellates in the South Atlantic Ocean during the late austral summer 1995, *Deep Sea Res., Part I*, 46, 451–482, 1999.
- Fleisher, M. Q., and R. F. Anderson, Assessing the collection efficiency of Ross Sea sediment traps using ^{230}Th and ^{231}Pa , *Deep Sea Res., Part II*, 50, 693–712, 2003.
- Francois, R., and M. P. Bacon, Variations in terrigenous input into the deep equatorial Atlantic during the past 24,000 years, *Science*, 251, 1473–1476, 1991.
- Francois, R., M. Bacon, and D. O. Suman, Thorium 230 profiling in deep-sea sediments: High-resolution records of flux and dissolution of carbonate in the equatorial Atlantic during the last 24,000 years, *Paleoceanography*, 5, 761–787, 1990.
- Gong, C., and D. J. Hollander, Evidence for differential degradation of alkenones under contrasting bottom water oxygen conditions: Implication for paleotemperature reconstruction, *Geochim. Cosmochim. Acta*, 63, 405–411, 1999.
- Goodney, D. E., S. V. Margolis, W. C. Dudley, P. Kroopnick, and D. F. Williams, Oxygen and carbon isotopes of recent calcareous nanofossils as paleoceanographic indicators, *Mar. Micropaleontol.*, 5, 31–42, 1980.
- Henderson, G. M., Seawater ($^{234}\text{U}/^{238}\text{U}$) during the last 800 thousand years, *Earth Planet. Sci. Lett.*, 199, 97–110, 2002.
- Henrichs, S. M., and W. S. Reebergh, Anaerobic mineralization of marine sediment organic matter: Rates and the role of anaerobic processes in the oceanic carbon economy, *Geomicrobiol. J.*, 5, 191–237, 1987.
- Herbert, T. D., Review of alkenone calibrations (culture, water column, and sediments), *Geochim. Geophys. Geosys.*, 2, Paper number 2000GC000055, 2001.
- Herbert, T. D., J. D. Schuffert, D. Thomas, C. Lange, A. Weinheimer, A. Peleo-Alampay, and J.-C. Herguera, Depth and seasonality of alkenone production along the California margin inferred from a core top transect, *Paleoceanography*, 13, 263–271, 1998.
- Hodell, D. A., C. D. Charles, and U. S. Ninnemann, Comparison of interglacial stages in the South Atlantic sector of the southern ocean for the past 450 kyr: Implications for Marine Isotope Stage (MIS) 11, *Global Planet. Change*, 24, 7–26, 2000.
- Hodell, D. A., C. D. Charles, J. H. Curtis, P. G. Mortyn, U. S. Ninnemann, and K. A. Venz, Data report: Oxygen isotope stratigraphy of ODP Leg 177 Sites 1088, 1089, 1090, 1093, and 1094, *Proc. Ocean Drill. Program, Sci. Results*, 177, 2001a. (Available at http://www-odp.tamu.edu/publications/177_SR/177sr.htm.)
- Hodell, D. A., C. D. Charles, and F. J. Sierro, Late Pleistocene evolution of the ocean's carbonate system, *Earth Planet. Sci. Lett.*, 192, 109–124, 2001b.
- Hoefs, M. J. L., G. J. M. Versteegh, W. I. C. Rijpstra, J. W. de Leeuw, and J. S. S. Damste, Postdepositional oxic degradation of alkenones: Implications for the measurement of palaeo sea surface temperatures, *Paleoceanography*, 17, 42–49, 1998.
- Howard, W. R., and W. L. Prell, Late Quaternary surface circulation of the southern Indian Ocean and its relationship to orbital variations, *Paleoceanography*, 7, 79–117, 1992.
- Jouzel, J., L. Merlivat, and C. Lorius, Deuterium excess in an east Antarctic ice core suggests higher relative humidity at the oceanic surface during the last glacial maximum, *Nature*, 299, 688–691, 1982.
- Keil, R. G., E. Tsamakidis, C. B. Fuh, J. C. Giddings, and J. I. Hedges, Mineralogical and textural controls on the organic composition of coastal marine sediments: Hydrodynamic separation using SPLITT-fractionation, *Geochim. Cosmochim. Acta*, 58, 879–893, 1994.
- Klinkhammer, G. P., and M. R. Palmer, Uranium in the oceans—Where it goes and why, *Geochim. Cosmochim. Acta*, 55, 1799–1806, 1991.
- Koster, R. D., J. Jouzel, R. J. Suozzo, and G. L. Russell, Origin of July Antarctic precipitation and its influence on deuterium content: A GCM analysis, *Clim. Dyn.*, 7, 195–203, 1992.
- Lea, D. W., Ice ages, the California Current, and Devil's Hole, *Science*, 293, 59–60, 2001.
- Lehman, S. J., J. P. Sachs, A. M. Crotwell, L. D. Keigwin, and E. A. Boyle, Relation of subtropical Atlantic temperature, high latitude ice rafting, deep water formation, and European climate 135,000–60,000 years ago, *Quat. Sci. Rev.*, 21, 1917–1924, 2002.
- Levitus, S., and T. Boyer, *World Ocean Atlas 1994*, vol. 4, *Temperature*, U.S. Dept. of Commerce, Washington, D. C., 1994.
- Martinson, D. G., N. G. Pisias, J. D. Hays, J. Imbrie, T. C. Moore, and N. J. Shackleton, Age dating and the orbital theory of the ice ages: Development of a high-resolution 0 to 300,000-year chronostratigraphy, *Quat. Res.*, 27, 1–29, 1987.
- Mortyn, P. G., Planktonic foraminifera and upper water column variability in the South Atlantic: A multiple species approach to the deep sea sedimentary record of climate change, Ph.D. thesis, Univ. of Calif., San Diego, La Jolla, Calif., 2000.
- Müller, P. J., M. Cepek, G. Ruhland, and R. R. Schneider, Alkenone and coccolithophorid species changes in Late Quaternary sediments from the Walvis Ridge: Implications for the alkenone paleotemperature method, *Palaeogeogr. Palaeoclimatol. Palaeoecol.*, 135, 71–96, 1997.
- Müller, P. J., G. Kirst, G. Ruhland, I. V. Storch, and A. Rosell-Mele, Calibration of the Alkenone paleotemperature index U_{37}^{Kl} based on core-tops from the eastern South Atlantic and the global ocean (60°N–60°S), *Geochim. Cosmochim. Acta*, 62, 1757–1772, 1998.
- Ninnemann, U. S., and C. D. Charles, Regional differences in Quaternary Subantarctic nutrient cycling: Link to intermediate and deep water ventilation, *Paleoceanography*, 12, 560–567, 1997.
- Ninnemann, U. S., C. D. Charles, and D. A. Hodell, Origin of global millennial scale climate events: Constraints from the Southern Ocean deep sea sedimentary record, in *Mechanisms of Global Climate Change*, edited by P. U. Clark, R. S. Webb, and L. D. Keigwin, pp. 99–112, AGU, Washington, D. C., 1999.

- Ohkouchi, N., T. I. Eglinton, L. D. Keigwin, and J. M. Hayes, Spatial and temporal offsets between proxy records in a sediment drift, *Science*, 298, 1224–1227, 2002.
- Prahl, F. G., and S. G. Wakeham, Calibration of unsaturation patterns in long-chain ketone compositions for palaeotemperature assessment, *Nature*, 330, 367–369, 1987.
- Prahl, F. G., L. A. Muehlhausen, and D. L. Zahnle, Further evaluation of long-chain alkenones as indicators of paleoceanographic conditions, *Geochim. Cosmochim. Acta*, 52, 2303–2310, 1988.
- Prahl, F. G., G. J. de Lange, M. Lyle, and M. A. Sparrow, Post-depositional stability of long-chain alkenones under contrasting redox conditions, *Nature*, 341, 434–437, 1989.
- Robinson, L. F., N. S. Belshaw, and G. M. Henderson, U and Th isotopes in seawater and modern carbonates from the Bahamas, *Geochim. Cosmochim. Acta*, in press, 2003.
- Sachs, J. P., and S. J. Lehman, Subtropical Atlantic temperatures 60,000 to 30,000 years ago, *Science*, 286, 756–759, 1999.
- Sachs, J. P., R. F. Anderson, and S. J. Lehman, Glacial surface temperatures of the southeast Atlantic Ocean, *Science*, 293, 2077–2079, 2001.
- Scholten, J. C., J. Fietzke, S. Vogler, M. M. Rutgers van der Loeff, A. Mangini, W. Koeve, J. Waniek, P. Stoffers, A. Antia, and J. Kuss, Trapping efficiencies of sediment traps from the deep eastern North Atlantic: The ^{230}Th calibration, *Deep Sea Res., Part II*, 48, 2383–2408, 2001.
- Spero, H. J., and D. W. Lea, The cause of carbon isotope minimum events on glacial terminations, *Science*, 296, 522–525, 2002.
- Stoner, J. S., J. E. T. Channell, C. Hillaire-Marcel, and C. Kissel, Geomagnetic paleointensity and environmental record from Labrador Sea core MD95-2024: Global marine sediment and ice core chronostratigraphy for the last 110 kyr, *Earth Planet. Sci. Lett.*, 183, 161–177, 2000.
- Suman, D. O., and M. P. Bacon, Variations in Holocene sedimentation in the North American Basin determined from ^{230}Th measurements, *Deep Sea Res.*, 36, 869–878, 1989.
- Teece, M. A., J. M. Getliff, J. W. Leftley, R. J. Parkes, and J. R. Maxwell, Microbial degradation of the marine prymnesiophyte *Emiliana huxleyi* under oxic and anoxic conditions as a model for early diagenesis: Long chain alkenones, alkenones and alkyl alkenoates, *Organic Geochem.*, 29, 863–880, 1998.
- Tucholke, B. E., and R. W. Embley, Cenozoic regional erosion of the abyssal sea floor off South, in *Interregional Unconformities and Hydrocarbon Accumulation*, edited by J. S. Schlee, pp. 145–164, Am. Assoc. of Petrol. Geol., Tulsa, Okla., 1984.
- Vimeux, F., V. Masson, J. Jouzel, M. Stievenard, and J. R. Petit, Glacial-interglacial changes in ocean surface conditions in the Southern Hemisphere, *Nature*, 398, 410–413, 1999.
- Yu, E. F., R. Francois, M. P. Bacon, and A. P. Fleer, Fluxes of ^{230}Th and ^{231}Pa to the deep sea: Implications for the interpretation of excess ^{230}Th and $^{231}\text{Pa}/^{230}\text{Th}$ profiles in sediments, *Earth Planet. Sci. Lett.*, 191, 219–230, 2001a.
- Yu, E. F., R. Francois, M. P. Bacon, S. Honjo, A. P. Fleer, S. J. Manganini, M. M. R. van der Loeff, and V. Ittekkot, Trapping efficiency of bottom-tethered sediment traps estimated from the intercepted fluxes of ^{230}Th and ^{231}Pa , *Deep Sea Res., Part I*, 48, 865–889, 2001b.
-
- R. F. Anderson, Geochemistry Building, Lamont-Doherty Earth Observatory, P.O. Box 1000, Palisades, NY 10964, USA. (boba@ldeo.columbia.edu)
- J. P. Sachs, Department of Earth, Atmospheric and Planetary Sciences, Massachusetts Institute of Technology, Cambridge, MA 02139, USA. (jsachs@mit.edu)